

Joint Demonstration and Preference Learning Improves Policy Alignment with Human Feedback

Chenliang Li, Siliang Zeng[†], Zeyi Liao[†], Jiaxiang Li,
Dongyeop Kang, Alfredo Garcia, Mingyi Hong*

June 12, 2024

Abstract

Aligning human preference and value is an important requirement for building contemporary foundation models and embodied AI. However, popular approaches such as reinforcement learning with human feedback (RLHF) break down the task into successive stages, such as supervised fine-tuning (SFT), reward modeling (RM), and reinforcement learning (RL), each performing one specific learning task. Such a sequential approach results in serious issues such as significant under-utilization of data and distribution mismatch between the learned reward model and generated policy, which eventually lead to poor alignment performance. We develop a *single stage* approach named Alignment with Integrated Human Feedback (AIHF), capable of integrating *both* human preference and demonstration to train reward models and the policy. The proposed approach admits a suite of efficient algorithms, which can easily reduce to, and leverage, popular alignment algorithms such as RLHF and Directly Policy Optimization (DPO), and only requires minor changes to the existing alignment pipelines. We demonstrate the efficiency of the proposed solutions with extensive experiments involving alignment problems in LLMs and robotic control problems in MuJoCo. We observe that the proposed solutions outperform the existing alignment algorithms such as RLHF and DPO by large margins, especially when the amount of high-quality preference data is relatively limited.

1 Introduction

Background. As ChatGPT has taken the world by storm, it is clear that AI systems will soon become ubiquitous in our lives. For instance, Large Language Models (LLMs) have been used to solve hard problems including video gaming [Berner et al., 2019, Mnih et al., 2015], autonomous control [Bellemare et al., 2020], and robotic manipulation [Kalashnikov et al., 2018, Kober and Peters, 2008]. However, for AI systems to be able to smoothly interact with humans, and reliably help perform mission-critical tasks, it is critical that the system learns, or aligns with, the human’s

*S. Zeng, J. Li and H. Hong are with Department of Electrical and Computer Engineering, University of Minnesota, Minneapolis, MN, USA. E-mails: zeng0176@umn.edu, li003755@umn.edu, mhong@umn.edu. Z. Liao is with the Department of Computer Science and Engineering, The Ohio State University, Columbus, OH, USA. E-mail: liao.629@osu.edu. D. Kang is with the Department of Computer Science and Engineering, University of Minnesota, Minneapolis, MN, USA. E-mail: dongyeop@umn.edu. C. Li and A. Garcia are with Department of Industrial and Systems Engineering, Texas A&M University, College Station, TX, USA. E-mails: chenliangli@tamu.edu, alfredo.garcia@tamu.edu.

[†]Equal contribution, orders determined by dice rolling.

preferred strategy, under specific contexts, and adapts to evolving user preferences and needs [Leike et al., 2018]. Achieving this level of *alignment* between AI and humans requires a comprehensive approach. AI systems must be capable of not only responding to instructions but also being sensitive to the nuances of human behavior and context, ensuring that their actions align with individual values and societal norms. On the other hand, various undesirable behaviors exhibited by advanced AI systems, e.g. deception [Park et al., 2023] and manipulation [Perez et al., 2022] have raised concerns about the potential hazards from AI systems.

The “alignment” task mentioned above has already proven to be useful in a few applications, such as in ChatGPT. Despite its recent popularity, the research area is still in its infancy. There are a number of critical open challenges, e.g. 1) How to solve the alignment problem leveraging diverse human feedback to further boost alignment performance? 2) How to enable AI systems to continuously learn and adapt to time-varying preferences, changing contexts, and emerging societal norms?

Contribution. In this work, we address the first question posed above. That is, we develop formulations and efficient algorithms capable of integrating different sources of human response data to achieve the best alignment performance.

Most of the existing alignment algorithms are *sequential*, i.e. they separate the alignment process into a number of successive stages, each utilizing one distinctive category of data. For example, the well-known RLHF approach adopted by [Ouyang et al., 2022] breaks the alignment step into the supervised finetuning (SFT), reward modeling (RM), and reinforcement learning (RL) stages, where the SFT stage uses demonstration data, the RM stage uses the preference data, and the RL stage uses a set of available prompts. Similar strategies have been used in other related works such as [Rafailov et al., 2023, Li et al., 2023, Zhu et al., 2023, Liu et al., 2023]. Sequencing of learning tasks may facilitate computation at the expense of inefficient exploitation of data. To illustrate, consider the three-stage RLHF approach proposed in [Ouyang et al., 2022], in the extreme case where the amount of high-quality preference data is quite limited, the reward model trained cannot adequately reflect the preferences of the human, which may lead to unsatisfactory performance in the RL stage. This simple example underscores the importance of ensuring the reward model is *consistent* with the policy model. Such consistency can not be guaranteed with sequential execution of the RM and RL tasks.

The alignment problem is a learning problem with (at least) three types of input data: the demonstration data (consists of prompts and human-generated continuations), the preference data (consists of prompts and pairs of human-ranked responses), as well as prompts without any responses. The input to the learning problem, besides these data, also includes a model pre-trained using a large corpus of text data. The output of the learning process is a fine-tuned model aligned with human preferences/values which govern the generation of demonstration and preference data. To integrate these diverse data, we propose a *joint* learning approach, which is informed by recent advances in Inverse Reinforcement Learning (IRL) [Arora and Doshi, 2021, Zeng et al., 2022b], stochastic choice theory [Blavatsky and Pogrebna, 2010] and bi-level optimization [Hong et al., 2020, Ji et al., 2021, Khanduri et al., 2021]. More specifically, the proposed formulation integrates SFT, RM, and RL into a single stage, so that reward modeling and policy optimization can *fully* leverage all three kinds of data mentioned above in alignment. Several existing alignment schemes, such as RLHF [Ouyang et al., 2022] and DPO [Rafailov et al., 2023], and some of their extensions can be seen as particular instances of the proposed formulation. We observe that the proposed solutions outperform the existing alignment algorithms such as RLHF by large margins, especially when the amount of

high-quality preference data is relatively limited.

2 Preliminaries and Related Work

2.1 Notation

The Finite-Horizon MDP Model. Consider a Markov decision process (MDP) defined by the tuple $(\mathcal{S}, \mathcal{A}, P, \rho, r, \gamma)$, which consists of the state space \mathcal{S} , the action space \mathcal{A} , the transition dynamics $P : \mathcal{S} \times \mathcal{A} \times \mathcal{S} \rightarrow [0, 1]$, the initial state distribution $\rho(\cdot)$, the reward function $r : \mathcal{S} \times \mathcal{A} \rightarrow \mathbb{R}$ and the discounted factor $\gamma > 0$. Let $s_t \in \mathcal{S}$, $a_t \in \mathcal{A}$ denote the state and action variables at time t respectively, where a_t is generated according to some policy $\pi(\cdot|s_t) : \mathcal{S} \rightarrow \Delta_{|\mathcal{A}|}$, where $\Delta_{|\mathcal{A}|}$ denotes the probability simplex in $\mathbb{R}^{|\mathcal{A}|}$. Note that viewing the generation process of language models as an MDP, s_t 's and a_t 's are referred to as the given sequence and next token to be generated, respectively; $\pi(\cdot)$ then represents the language model itself. Define $\tau := \{(s_t, a_t)\}_{t=1}^T$ as a (finite time) trajectory of state and action pairs. Let $\mathcal{H}_T \subset \prod_{t=0}^{T-1} (\mathcal{S} \times \mathcal{A})$ denote all feasible state/action pairs.

Human Feedback Generation. Assume that the human demonstration τ is generated from a ground-truth *human expert* policy π^E , i.e., for each state s_t , we have $a_t \sim \pi^E(\cdot|s_t)$. Moreover, let ' $\tau_l \prec \tau_w$ ' indicate the winner trajectory τ_w is preferred over the trajectory τ_l . Further, we denote $(\tau_l \prec \tau_w) \sim \pi^P$ as the preference oracle.

Note that when we present our *problem formulation*, we will use the above data generation distributions so quantities such as *likelihood* can be properly defined. *Finite-sample* version of demonstration and preference data will be introduced subsequently to facilitate algorithm design.

Since reward modeling is a critical task for achieving state-of-the-art alignment performance, below we review a few popular paradigms for reward learning.

2.2 Reward Learning from Preference Data

RLHF is a popular technique for finetuning AI systems to align with human preferences and values. The RLHF approach proposed in [Stiennon et al., 2020, Ouyang et al., 2022] consists of the following three-stage: 1) the **supervised fine-tuning (SFT)** stage, where the demonstration data is used to fine-tune the model in a supervised manner; 2) the **reward modeling (RM)** stage, where the preference data is used to train a reward model; 3) the **reinforcement learning (RL)** stage, where the SFT model is further finetuned by running RL using the trained reward model.

Furthermore, existing work such as Direct Preference optimization (DPO) [Rafailov et al., 2023] and Inverse Preference Learning (IPL) [Hejna and Sadigh, 2023] both remove the need for explicit reward modeling, and they directly extract the policy from preferences. This greatly reduces the training complexity, but it has been observed that these algorithms can be unstable in the training process [Azar et al., 2023, Xu et al., 2024]. There is also a large number of works that aim to learn reward functions from rating [Daniel et al., 2014] or ranking [Yuan et al., 2023, Myers et al., 2022]. However, these works often fail when the quality of the preference dataset is low Morimura et al. [2024]. In our approach, the inclusion of additional demonstrations can be leveraged to counteract the adverse effects of limited preference quality.

2.3 Reward Learning using Demonstration Data

In the RL literature, a line of work referred to as Inverse Reinforcement Learning (IRL) proposes to *jointly* learn the reward and policy from expert demonstration data. Specifically, the target is to find the parameterized reward function $r(s, a; \theta)$ (resp. an optimal policy $\pi^*(s, a)$) that best explains (resp. mimics) an expert policy π^E given the demonstration data \mathcal{D} . For example, the well-known maximum entropy IRL (MaxEnt-IRL) framework [Ziebart, 2010, Ziebart et al., 2013, Bloem and Bambos, 2014, Zhou et al., 2017] finds a policy maximizing entropy subject to the expected features that match the empirical averages in the expert’s observation dataset. However, this approach can only be used to model linear rewards.

Subsequent works such as [Levine et al., 2011, Wulfmeier et al., 2015, Zeng et al., 2022b] further improve the MaxEnt-IRL method so that nonlinear reward can be used. For example, a recent paper [Zeng et al., 2022a] proposed a maximum likelihood IRL (ML-IRL) formulation based on the Dynamic Discrete Choice (DDC) model, and nonlinear reward function can be used. It is also shown that when the reward function is linearly parameterized, then the MaxEnt is the Lagrangian dual of the ML-IRL problem. However, it is worth mentioning that to our best knowledge, almost all IRL-based methods can only utilize demonstration data, which can be problematic because a large amount of high-quality demonstration data is typically hard to obtain. Further, it is well-known that only using demonstration cannot extract precise human preference, especially in safety-related tasks where the boundaries between permissible and impermissible actions need to be precisely determined [Liao and Sun, 2024]; see, e.g., [Fischer et al., 2021] which shows that insufficient demonstration dataset could lead to high generalization error.

2.4 Reward Learning from Diverse Data

For a more precise alignment of agent behavior with human intention, it is crucial to leverage diverse data source such as *both* expert demonstrations and human feedback to achieve alignment. In [Ibarz et al., 2018], the authors first combine two approaches to learn from human feedback: expert demonstrations and trajectory preferences. The addition of demonstrations to learning from preferences typically results in substantial performance gains compared with using either demonstrations or preferences in isolation. In [Palan et al., 2019] and [Biyik et al., 2022], the authors integrate diverse sources of human feedback including demonstrations and pairwise comparisons in a Bayesian approach to learn reward functions that are assumed to be linear in carefully selected features and evaluate their proposed method on robot learning platform. Moreover, their proposed methods need to actively generate preference queries, which are expensive to collect in practical applications. In contrast, our proposed approach (to be presented shortly) is not Bayesian and does not include the requirement that the reward model is linear in pre-selected features. Hong et al. [2024] proposed a single-stage supervised learning algorithm ORPO that can perform supervised fine-tuning and preference alignment in one training session without maintaining multiple models simultaneously. However, Hong et al. [2024] can suffer from overoptimization due to its supervised learning pipeline Liu et al. [2024].

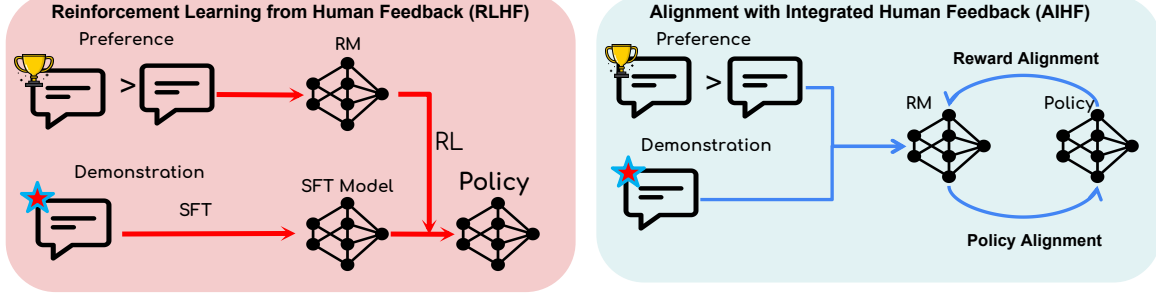


Figure 1: Comparison of the RLHF with the proposed AIHF.

3 Proposed Approach: Alignment with Integrated Human Feedback (AIHF)

3.1 Preliminaries

In this section, we develop our proposed formulation for the alignment problem. To flesh out our ideas, let us start with a brief discussion of the RLHF approach. First, the SFT stage maximizes the following likelihood function:

$$\ell_{\text{SFT}}(\pi) := \mathbb{E}_{\tau \sim \pi^{\text{E}}} \left[\log \prod_{t \geq 0} \left(\pi(a_t | s_t) \right)^{\gamma^t} \right]. \quad (1)$$

For the RM stage, let $R(\tau; \theta) := \sum_{t \geq 0} \gamma^t r(s_t, a_t; \theta)$ denote the (parameterized) discounted cumulative reward of one trajectory τ . Following the Bradley-Terry-Luce (BTL) model [Bradley and Terry, 1952], the human preference distribution for one pair of trajectories can be stipulated as (where $\sigma(\cdot)$ is the sigmoid function):

$$P[\tau_l \prec \tau_w] = \sigma(R(\tau_w; \theta) - R(\tau_l; \theta)). \quad (2)$$

Based on (2), this stage maximizes the following:

$$\ell_{\text{RM}}(\theta) := \mathbb{E}_{(\tau_l \prec \tau_w) \in \pi^P} \left[\log \left(\sigma(R(\tau_w; \theta) - R(\tau_l; \theta)) \right) \right]. \quad (3)$$

Finally, the RL stage fine-tunes the SFT policy by solving the following policy optimization problem:

$$\max_{\pi} \ell_{\text{RL}}(\pi; R(\cdot; \theta)) := \mathbb{E}_{s_0 \sim \rho, \tau \sim \pi} \left[R(\tau; \theta) + \sum_{t \geq 0} \gamma^t c(\pi) \right] \quad (4)$$

where $c(\pi)$ is a penalty function, which can take the form of, e.g., the KL divergence $c(\pi) := D_{\text{KL}}(\pi(\cdot | s_t) \| \pi_{\text{SFT}}(\cdot | s_t))$. This penalty ensures the resulting policy is close to the original SFT policy. We have the following remark about the above problem.

Remark 3.1 (Optimal Policy for RLHF) Let π_{θ} denote the optimal policy for problem (4), where θ is used to parameterize the reward function. When $c(\pi) := D_{\text{KL}}(\pi(\cdot | s_t) \| \pi_{\text{SFT}}(\cdot | s_t))$, the

KL-regularized MDP problem described by (4) has a closed-form solution:

$$\pi_\theta(a|s) = \frac{\pi_{\text{SFT}}(a|s) \exp(Q_\theta(s, a)/\beta)}{\sum_{\tilde{a}} \pi_{\text{SFT}}(\tilde{a}|s) \exp(Q_\theta(s, \tilde{a})/\beta)}, \quad (5)$$

where the corresponding value function V_θ and the Q-function Q_θ are defined as below:

$$V_\theta(s) := \mathbb{E}_{\tau \sim \pi_\theta} \left[R(\tau; \theta) + \beta \sum_{t=0}^{\infty} \gamma^t D_{\text{KL}} \left(\pi(\cdot|s_t) \parallel \pi_{\text{SFT}}(\cdot|s_t) \right) \middle| s_0 = s \right] \quad (6a)$$

$$Q_\theta(s, a) := r(s, a; \theta) + \gamma \mathbb{E}_{s' \sim P(\cdot|s, a)} [V_\theta(s')]. \quad (6b)$$

Further, assuming that $T = 1$, i.e., $\tau = (s_0, a_0)$, and considering the LLM alignment problem as a sequence-level training problem (this is a popular simplification in language models, see, e.g., Rafailov et al. [2023]), the closed-form expression of π_θ (5) can be reduced to:

$$\pi_\theta(a_t|s_t) = \frac{\pi_{\text{SFT}}(a_t|s_t) \exp(\frac{1}{\beta} r(a_t, s_t; \theta))}{\sum_{a_t \in A} (\pi_{\text{SFT}}(a_t|s_t) \exp(\frac{1}{\beta} r(a_t, s_t; \theta)))}. \quad (7)$$

Remark 3.2 (Interpretation of the RLHF Policy) Let us take a closer look at (7). In this expression, the results of learning from demonstration data (i.e., $\pi_{\text{SFT}}(\cdot)$) and from the preference data (i.e., $r(\cdot; \theta)$) are combined together in a product form to yield the final policy estimate. Such a form, though convenient, can result in a number of issues.

One such an issue is that, the reward $R(\tau; \theta)$ is learned only through the preference dataset \mathcal{P} . Despite the fact that problem (3) is relatively simple to optimize, such an approach has the following issues: 1) the high-quality demonstration data has been ignored in shaping the reward model; 2) in the situation where the preference data has limited coverage or is of low-quality, the learned reward model is likely to be of low quality as well. Here, *low-quality* preference data arises when, e.g., the trajectories are generated from low-quality models, or the preference annotation is noisy.

To see the impact on the noisy annotation, consider, for example, the case where a given s_t , suppose there are two actions \hat{a}_t and \tilde{a}_t , and they are equally good. The SFT data respects the ground truth, and the learned SFT policy says $\pi_{\text{SFT}}(\tilde{a}_t|s_t) \approx \pi_{\text{SFT}}(\hat{a}_t|s_t)$. However, due to labeling noise, we have a preference data $(s_t, \hat{a}_t) \prec (s_t, \tilde{a}_t)$, therefore we have learned $R(a_t, \tilde{a}_t; \theta) > R(a_t, \hat{a}_t; \theta)$, yielding significant difference in the final policy. We refer the readers to Sec. 4 for more discussion.

3.2 A Meta-Formulation

The above discussion strongly motivates us to develop an approach that can model the *entire* alignment process with a common parametrization for both policy and reward models. Towards this end, let us consider the following *meta*-formulation:

$$(\text{AIHF}) \quad \max_{\theta} \quad L(\theta) := \alpha L_1(\pi_\theta) + L_2(R(\cdot; \theta)) \quad (8a)$$

$$\text{s.t.} \quad \pi_\theta := \arg \max_{\pi} L_3(\pi; R(\cdot; \theta)) \quad (8b)$$

where $\theta \in \mathbb{R}^d$ is a parameter; $L_1(\pi_\theta)$ is a measure of fit of the parameterized policy π_θ to demonstration data and $L_2(R(\cdot; \theta))$ is a measure of fit of the parameterized reward model $R(\cdot; \theta)$ to the preference data; $L_3(\pi, R(\cdot; \theta))$ is a measure of performance of policy π with respect to reward model $R(\cdot; \theta)$;

$\alpha \geq 0$ is a balancing coefficient reflecting the relative size of demonstration versus preference data. We refer the above formulation as Alignment with Integrated Human Feedback (AIHF); see Fig. 1 for an illustration of the proposed formulation. The AIHF (8) is a *meta*-problem that models the alignment problem. It has two levels: an upper-level problem in which the goal is to find policy and reward models that jointly maximize a measure of fit to demonstrations and preference datasets and a lower-level problem which ensures that the policy model optimizes performance with respect to the reward model. Its components can be customized to yield specific alignment formulations and algorithms. But before diving into various customizations, let us discuss the advantages of this formulation.

Generality. One can specialize the choice of loss functions and problem parameters, to yield a number of existing alignment formulations. Such generality implies that algorithms developed for (8) are easily applicable to different special formulations it covers. For more details see Sec. 3.4.

Joint optimization. The formulation jointly optimizes the reward and the policy. One benefit here is that it can strengthen the reward model through integrating both demonstrations and pairwise comparisons. Compared with the standard RLHF pipeline, through integrating additional data source such as demonstrations to train the reward model, it can further boost the policy optimization subroutine to achieve better alignment performance. See Sec. 5 for a detailed discussion on how the reward parameter θ is updated by leveraging such demonstration.

Dataset Integration. Clearly, the reward learning process leverages all the available data, therefore, we can expect that a high-quality reward model can still be obtained even under unfavorable situations where certain category of data is scarce or of low quality.

3.3 Specification of AIHF

In this section, we specify the formulation (8). Let us begin with the choice of L_1 . It can be directly instantiated by using an objective similar to (1), which is the likelihood function over the collected expert demonstrations. Note that we aim to optimize the reward parameter θ to align with human feedback in (8a), thus the objective of L_1 can be specialized as a maximum likelihood function over expert demonstrations as below:

$$L_1(\pi_\theta) := \mathbb{E}_{\tau \sim \pi^E} \left[\sum_{t=0}^{\infty} \gamma^t \log \pi_\theta(a_t | s_t) \right]. \quad (9)$$

Here π_θ optimizes the measure of performance $L_3(\pi; R(\cdot; \theta))$ for a reward model $R(\cdot; \theta)$ as below:

$$L_3(\pi; R(\cdot; \theta)) := \mathbb{E}_{s_0 \sim \rho, \tau \sim \pi} \left[R(\tau; \theta) - \beta \sum_{t \geq 0} \gamma^t D_{\text{KL}} \left(\pi(\cdot | s_t) \| \pi^0(\cdot | s_t) \right) \right] \quad (10)$$

where π^0 is some initial policy and $\beta > 0$ is temperature parameter.

Next, we specify L_2 . To ensure internal model consistency, we identify the likelihood function for preference data so it is in accordance with the preferences implied by the reward model $R(\cdot; \theta)$ used in the definitions of L_1 and L_3 . Thus, the optimal distribution μ_θ over the set of T -long sequence of state-action pairs is defined as follows:

$$\mu_\theta := \arg \max_{\mu \in \Delta^T} \mathbb{E}_{\tau \sim \mu} [R(\tau; \theta) - \beta \mathcal{D}_{\text{KL}}(\mu \| \mu^0)]$$

where Δ_T denotes the simplex on \mathcal{H}_T and μ^0 is a prior distribution on the trajectories. It can be shown the solution of the above problem is of the form:

$$\mu_\theta(\tau) = \frac{\mu^0(\tau) \exp(R(\tau; \theta)/\beta)}{\sum_{\tau' \in \mathcal{H}_T} \mu^0(\tau') \exp(R(\tau'; \theta)/\beta)}.$$

With this result, we can now obtain a model for the likelihood that sequence τ_j is preferred over τ_i . By the *independence of irrelevant alternatives* property [Fudenberg et al., 2015] of the optimal choice μ_θ , when the set of feasible choices is reduced from \mathcal{H}_T to just the two-tuple $\{\tau_i, \tau_j\}$, the likelihood that sequence τ_j is preferred over τ_i is given by $\mathbb{P}_\theta(\tau_i \prec \tau_j) := \frac{\mu_\theta(\tau_j)}{\mu_\theta(\tau_i) + \mu_\theta(\tau_j)}$. This motivates the choice of $L_2(\theta)$ as the following *likelihood function*:

$$L_2(R(\cdot; \theta)) = \mathbb{E}_{(\tau_i \prec \tau_j) \in \pi^P} \left[\log \frac{\mu_\theta(\tau_j)}{\mu_\theta(\tau_j) + \mu_\theta(\tau_i)} \right] = \mathbb{E}_{(\tau_i \prec \tau_j) \in \pi^P} \left[\log \frac{\mu^0(\tau_j) \exp(R(\tau_j; \theta))}{\mu^0(\tau_j) \exp(R(\tau_j; \theta)) + \mu^0(\tau_i) \exp(R(\tau_i; \theta))} \right].$$

With μ^0 equal to the uniform distribution on \mathcal{H}_T , this model is equivalent to the BTL model (3):

$$L_2^{\text{BTL}}(\theta) = \ell_{\text{RM}}(\theta) = \mathbb{E}_{(\tau_i \prec \tau_j) \in \pi^P} \left[\log \left(\sigma(R(\tau_j; \theta) - R(\tau_i; \theta)) \right) \right]. \quad (11)$$

3.4 Special Cases of AIHF

Next we discuss how formulation (8) can be specialized to some of the known alignment algorithms.

Specialization to RLHF-Type Approach. First, if we set the coefficient $\alpha = 0$ in (8), we obtain the following problem:

$$\max_{\theta} L_2(\theta) \text{ s.t. } \pi_\theta := \arg \max_{\pi} L_3(\pi; R(\cdot; \theta)). \quad (12)$$

We note that now the upper- and lower-level problems are completely decomposable, since the upper-level problem solves for the reward parameterization θ , while the lower-level problem solves for the policy (for the given reward), yielding two separate problems, which are exactly the RM and the RL problems in the typical RLHF approach.

Specialization to DPO-Type Approach. Let us consider the relationship between our formulation (8) with the DPO-type approaches. Let us set the following objective function $L_1 = \ell_{\text{SFT}}$ and $L_2 = \ell_{\text{RM}}$, and assume that $T = 1$ for the generation process. Through relaxing the constraint which ensures the policy is optimal w.r.t. a certain parameterized model, we can obtain a DPO-type formulation:

$$\max_{\pi} L(\pi) := \alpha \cdot \mathbb{E}_{\tau^E \sim \pi^E} \left[\log \pi(a^E | s^E) \right] + \mathbb{E}_{(\tau_i \prec \tau_j) \sim \pi^P} \left[\sigma \left(\beta \log \frac{\pi(a_j | s_j)}{\pi^0(a_i | s_j)} - \beta \log \frac{\pi(a_i | s_i)}{\pi^0(a_j | s_i)} \right) \right]. \quad (13)$$

The above formulation specializes to Liu et al. [2024], which is a slightly generalized version of DPO when *both* demonstration and preference data are used. Setting $\alpha = 0$ reduces to the problem solved by DPO; see Rafailov et al. [2023], Eq. (2).

4 Why AIHF can outperform two-stage alignment approaches?

To understand the difference between the proposed approach and the two-stage approach of the standard alignment pipeline, let us consider the following thought process over a simplified, but informative setting.

Let us consider the simplified case where there are N discrete actions, that is, the action set is $A := \{\tau_1, \tau_2, \dots, \tau_N\}$. Assume that there is a reward function $r(\cdot) : A \mapsto \mathbb{R}$ (note, that here the parameterization of the reward has been omitted for simplicity). Let us compare the optimal solutions for different alignment algorithms and get some intuition about each approach. Throughout the process, we will assume that the reward function is *not* parameterized, and we *directly* learn the optimal reward value. Indeed this is a simplification needed to understand the structure of the solution, but we argue that this is without loss of generality, since if the reward model is sufficiently parameterized by neural networks, then these optimal reward values can always be recovered by proper training.

Consider the following decision-making model:

$$\pi^* := \arg \max_{\pi \in \Delta^N} \mathbb{E}_{\tau \sim \pi(\cdot)} [r(\tau) - \beta \log \pi(\tau)], \quad (14)$$

where Δ^N is the probability simplex and $\beta > 0$. It can be shown that the solution to (14) is:

$$\pi_i^*(r) = \frac{\exp(\frac{r_i}{\beta})}{\sum_j \exp(\frac{r_j}{\beta})}, \quad \text{where } r_i := r(\tau_i), \quad \forall i. \quad (15)$$

Reward Estimation via Demonstration Data: When demonstration data $\mathcal{D} := \{\tau_n\}$ is available where each $\tau_n \in A$, $\forall n$, the estimation problem can be written as:

$$\hat{r}_{\mathcal{D}} := \arg \max_r \ell_{\mathcal{D}}(r)$$

where $\ell_{\mathcal{D}}(r) := \mathbb{E}_{\tau_i \sim \mathcal{D}} [\log \pi_i^*(r)]$. By (15) it follows that

$$\ell_{\mathcal{D}}(r) = \frac{1}{\beta} \mathbb{E}_{\tau_i \sim \mathcal{D}} [r_i] - \log \sum_j \exp(\frac{r_j}{\beta}).$$

Hence, it is easy to verify the gradient is:

$$\frac{\partial \ell_{\mathcal{D}}(r)}{\partial r_i} = \frac{1}{\beta} \left(\frac{\#\tau_i \text{ in } \mathcal{D}}{|\mathcal{D}|} - \pi_i^*(r) \right), \quad \forall i. \quad (16)$$

and the second order derivatives are:

$$\frac{\partial^2 \ell_{\mathcal{D}}(r)}{\partial r_i^2} = -\frac{1}{\beta^2} \pi_i^*(r)(1 - \pi_i^*(r)) \quad \frac{\partial^2 \ell_{\mathcal{D}}(r)}{\partial r_i \partial r_j} = \frac{1}{\beta^2} \pi_i^*(r) \pi_j^*(r). \quad (17)$$

Therefore, we can observe that setting the gradient to zero, the first-order stationary solution (in fact, in this case it is optimal solution since the Hessian is negative definite) indicates that the estimate of the probability of choosing action i is equal to the observed frequency of action τ_i appears in \mathcal{D} .

Note that in our simplified case, the above estimator can be viewed as the counterpart for the SFT estimator since it is the best that one can get using only demonstration data.

Reward Estimation with Preferences Data: Suppose that the preference data is available, $\mathcal{P} := \{(\tau_i \prec \tau_j)\}$, where again $\tau_i, \tau_j \in A$. Let us understand how to analyze the optimal policy π^* .

By IIA (independence of irrelevant alternatives) [Fudenberg et al., 2015], when the decision maker is asked to choose between only two alternatives $\{\tau_i, \tau_j\}$, we have :

$$\Pr(\tau_j \prec \tau_i) = \frac{\pi_i^*(r)}{\pi_i^*(r) + \pi_j^*(r)}.$$

The reward estimation problem is defined as:

$$\hat{r}_{\mathcal{P}} \in \arg \max_r \ell_{\mathcal{P}}(r) \quad (18)$$

where $\ell_{\mathcal{P}}(r) := \mathbb{E}_{(\tau_j \prec \tau_i) \sim \mathcal{P}} \left[\log \frac{\pi_i^*(r)}{\pi_i^*(r) + \pi_j^*(r)} \right]$. The partial derivative of the log-likelihood is given by:

$$\frac{\partial \ell_{\mathcal{P}}(r)}{\partial r_i} = \frac{1}{\beta} \sum_{j \neq i} \left(\frac{\#\{\tau_j \prec \tau_i \text{ in } \mathcal{P}\}}{|\mathcal{P}_{i,j}|} - \frac{\pi_i^*(r)}{\pi_i^*(r) + \pi_j^*(r)} \right) \frac{|\mathcal{P}_{i,j}|}{|\mathcal{P}|}. \quad (19)$$

The first-order condition can be written as:

$$\pi_i^*(r) = \frac{\sum_{j \neq i} \{\#a_i \succ a_j \text{ in } \mathcal{P}\}}{\sum_{j \neq i} |\mathcal{P}_{i,j}| \rho_{-(i,j)}^*(r)} \quad (20)$$

where $\rho_{-(i,j)}^*(r) := \left(1 - \sum_{k \in A \setminus \{i,j\}} \pi_k^*(r) \right)^{-1}$ is the expected number of times an action *other* than τ_i or τ_j is selected when sampling $\pi^*(r)$ infinitely many times. The second-order derivatives are given by

$$\frac{\partial^2 \ell_{\mathcal{P}}(r)}{\partial r_i^2} = -\frac{1}{\beta^2} \sum_{j \neq i} \frac{\pi_i^*(r)}{\pi_i^*(r) + \pi_j^*(r)} \frac{\pi_j^*(r)}{\pi_i^*(r) + \pi_j^*(r)} \frac{|\mathcal{P}_{i,j}|}{|\mathcal{P}|} \quad \frac{\partial^2 \ell_{\mathcal{P}}(r)}{\partial r_j \partial r_i} = \frac{1}{\beta^2} \frac{\pi_i^*(r)}{\pi_i^*(r) + \pi_j^*(r)} \frac{\pi_j^*(r)}{\pi_i^*(r) + \pi_j^*(r)} \frac{|\mathcal{P}_{i,j}|}{|\mathcal{P}|}.$$

Note that compared with the previous case with only demonstration data, here the first-order solution does not imply global optimality since the Hessian is not negative semi-definite.

Next, by using the above analysis, let us understand the policies that can be obtained by different alignment algorithms.

SFT Estimator. In this case, it is easy to observe that the optimal policy is given by

$$\pi_i^{\text{SFT}} = \frac{\#\tau_i \text{ in } \mathcal{D}}{|\mathcal{D}|} = \pi^*(\hat{r}_{\mathcal{D}}), \forall i. \quad (21)$$

RLHF Policy. The RLHF policy is defined as follows:

$$\pi^{\text{RLHF}} = \arg \max_{\pi \in \Delta^N} \mathbb{E}_{\tau_i \sim \pi} [\hat{r}_{\mathcal{P}}(\tau_i)] - \beta \text{KL}(\pi || \pi^{\text{SFT}})$$

where $\hat{r}_{\mathcal{P}}$ is the estimator obtained from preferences (i.e. solution to (20)), π^{SFT} is a prior distribution obtained from the SFT model trained with demonstration dataset \mathcal{D} , and Δ^N is the probability

simplex. It follows that

$$\begin{aligned}
\pi^{\text{RLHF}}(\tau_i) &= \frac{\pi^{\text{SFT}}(\tau_i) \exp \frac{1}{\beta} \hat{r}_{\mathcal{P}}(\tau_i)}{\sum_{j=1}^n \pi^{\text{SFT}}(\tau_j) \exp \frac{1}{\beta} \hat{r}_{\mathcal{P}}(\tau_j)} \\
&= \frac{\exp \frac{1}{\beta} \hat{r}_{\mathcal{D}}(\tau_i) \exp \frac{1}{\beta} \hat{r}_{\mathcal{P}}(\tau_i)}{\sum_{j=1}^n \exp \frac{1}{\beta} \hat{r}_{\mathcal{D}}(\tau_j) \exp \frac{1}{\beta} \hat{r}_{\mathcal{P}}(\tau_j)} \\
&= \frac{\exp \left(\frac{1}{\beta} (\hat{r}_{\mathcal{D}}(\tau_i) + \hat{r}_{\mathcal{P}}(\tau_i)) \right)}{\sum_{j=1}^n \exp \left(\frac{1}{\beta} (\hat{r}_{\mathcal{D}}(\tau_j) + \hat{r}_{\mathcal{P}}(\tau_j)) \right)} \\
&= \pi_i^* \left(\hat{r}_{\mathcal{D}} + \hat{r}_{\mathcal{P}} \right)
\end{aligned} \tag{22}$$

That is, the RLHF policy can be seen as the softmax policy for the *sum* of reward estimators.

AIHF estimator: In AIHF, assume that the lower-level problem uses (10), and the prior π^0 is uniform, then the optimal π^{AIHF} follows the same expression as in (15). One can then plug in such a solution to its loss function in (8a), and obtain the following reward learning problem:

$$\hat{r}^{\text{AIHF}} = \arg \max_r \ell_{\mathcal{D}+\mathcal{P}}(r) := |\mathcal{D}|L_1(r) + |\mathcal{P}|L_2(r) \tag{23}$$

where $L_1(r) := \mathbb{E}_{\tau_i \sim \mathcal{D}}[\log \pi_i^*(r)]$ and $L_2(r) := \mathbb{E}_{(\tau_j \prec \tau_i) \sim \mathcal{P}}[\log \frac{\pi_i^*(r)}{\pi_i^*(r) + \pi_j^*(r)}]$.

Using (16) and (19), we obtain:

$$\frac{\partial \ell_{\mathcal{D}+\mathcal{P}}(r)}{\partial r_i} = \frac{\#\{\tau_i \text{ in } \mathcal{D}\}}{|\mathcal{D}|} |\mathcal{D}| + \sum_{j \neq i} \#\{\tau_j \prec \tau_i \text{ in } \mathcal{P}\} - \pi_i^* |\mathcal{D}| - \sum_{j \neq i} \frac{\pi_i^*(r)}{\pi_i^*(r) + \pi_j^*(r)} |\mathcal{P}_{i,j}|.$$

Hence, the first-order condition is:

$$\#\{\tau_i \text{ in } \mathcal{D}\} + \sum_{j \neq i} \#\{\tau_j \prec \tau_i \text{ in } \mathcal{P}\} = \pi_i^*(r) (|\mathcal{D}| + \sum_{j \neq i} |\mathcal{P}_{i,j}| \frac{1}{\pi_i^*(r) + \pi_j^*(r)})$$

Or equivalently,

$$\pi_i^*(r) = \frac{\#\{a_i \text{ in } \mathcal{D}\} + \sum_{j \neq i} \#\{a_j \prec a_i \text{ in } \mathcal{P}\}}{|\mathcal{D}| + \sum_{j \neq i} |\mathcal{P}_{i,j}| \rho_{-(i,j)}^*(r)}. \tag{24}$$

Example 1: With $\beta = 1$ and only two actions τ_1 and τ_2 . Since $\rho^*(r)_{-(1,2)} = 1$, it follows that:

$$\begin{aligned}
\pi_1^{\text{AIHF}} &:= \pi_1^*(\hat{r}^{\text{AIHF}}) = \frac{\#\{\tau_1 \text{ in } \mathcal{D}\} + \#\{\tau_2 \prec \tau_1 \text{ in } \mathcal{P}\}}{|\mathcal{D}| + |\mathcal{P}|} \\
&= \frac{|\mathcal{D}|}{|\mathcal{D}| + |\mathcal{P}|} \pi_1^*(\hat{r}_{\mathcal{D}}) + \frac{|\mathcal{P}|}{|\mathcal{D}| + |\mathcal{P}|} \pi_1^*(\hat{r}_{\mathcal{P}}).
\end{aligned}$$

That is, the policy estimate obtained by using demonstrations and preferences is a *weighted* average of the policies estimated by using only demonstrations and only preferences. Slightly abusing notations, let $\pi_1^* := \pi_1^*(r^*)$ where r^* is the ground-truth reward. It follows that $\text{Var}(\pi_1^*(\hat{r}_{\mathcal{D}})) = \frac{\pi_1^*(1-\pi_1^*)}{|\mathcal{D}|}$, $\text{Var}(\pi_1^*(\hat{r}_{\mathcal{P}})) = \frac{\pi_1^*(1-\pi_1^*)}{|\mathcal{P}|}$ and

$$\text{Var}(\pi_1^{\text{AIHF}}) = \frac{\pi_1^*(1-\pi_1^*)}{|\mathcal{D}| + |\mathcal{P}|}.$$

This shows the AIHF policy estimator has *less variance* than either one of the estimators obtained from demonstrations *only* or preferences *only*.

To further illustrate, suppose $r(\tau_1) = r(\tau_2)$ and we have the following datasets:

$$\#\{\tau_1 \text{ in } \mathcal{D}\} = \#\{\tau_2 \text{ in } \mathcal{D}\} = 50, \quad \#\{\tau_1 \succ \tau_2 \text{ in } \mathcal{P}\} = 6, \quad \#\{\tau_2 \succ \tau_1 \text{ in } \mathcal{P}\} = 4.$$

With the given data, $\pi_1^{\text{SFT}} = \pi_1^*(\hat{r}_{\mathcal{P}}) = \frac{\#\{\tau_1 \text{ in } \mathcal{D}\}}{|\mathcal{D}|} = \frac{50}{100}$ and the solution to (20) yields

$$\pi_1^*(\hat{r}_{\mathcal{P}}) = \frac{\exp \hat{r}_{\mathcal{P}}(\tau_1)}{\exp \hat{r}_{\mathcal{P}}(\tau_1) + \exp \hat{r}_{\mathcal{P}}(\tau_2)} = \frac{6}{10}$$

Hence, $\pi_1^{\text{AIHF}} = \frac{100}{10+100}\pi_1^*(\hat{r}_{\mathcal{D}}) + \frac{10}{10+100}\pi_1^*(\hat{r}_{\mathcal{P}}) = \frac{56}{110}$. It follows from (22) that:

$$\begin{aligned} \pi_1^{\text{RLHF}} &= \frac{\pi_1^{\text{SFT}} \exp \hat{r}_{\mathcal{P}}(\tau_1)}{\pi_1^{\text{SFT}} \exp \hat{r}_{\mathcal{P}}(\tau_1) + \pi_2^{\text{SFT}} \exp \hat{r}_{\mathcal{P}}(\tau_2)} \\ &= \frac{\exp \hat{r}_{\mathcal{P}}(\tau_1)}{\exp \hat{r}_{\mathcal{P}}(\tau_1) + \exp \hat{r}_{\mathcal{P}}(\tau_2)} = \frac{6}{10}. \end{aligned}$$

In this example, the RLHF policy estimator is the farthest from ground-truth, because it does not correctly use the information provided by the demonstration data which in this case happens by chance to be correct $\pi_1^{\text{SFT}} = \pi_1^*(\hat{r}_{\mathcal{P}}) = \frac{1}{2}$.

As a second example, again suppose $r(\tau_1) = r(\tau_2)$. Consider now the datasets:

$$\{\#\tau_1 \text{ in } \mathcal{D}\} = 6, \quad \{\#\tau_2 \text{ in } \mathcal{D}\} = 4, \quad \{\#\tau_1 \succ \tau_2 \text{ in } \mathcal{P}\} = \{\#\tau_2 \succ \tau_1 \text{ in } \mathcal{P}\} = 50. \quad (25)$$

In this case, $\pi_1^{\text{SFT}} = \pi_1^*(\hat{r}_{\mathcal{P}}) = \frac{6}{10}$ and the solution to (20) yields

$$\pi_1^*(\hat{r}_{\mathcal{P}}) = \frac{\exp \hat{r}_{\mathcal{P}}(\tau_1)}{\exp \hat{r}_{\mathcal{P}}(\tau_1) + \exp \hat{r}_{\mathcal{P}}(\tau_2)} = \frac{50}{100}.$$

It follows from (22) that:

$$\begin{aligned} \pi_1^{\text{RLHF}} &= \frac{\pi_1^{\text{SFT}} \exp \hat{r}_{\mathcal{P}}(\tau_1)}{\pi_1^{\text{SFT}} \exp \hat{r}_{\mathcal{P}}(\tau_1) + \pi_2^{\text{SFT}} \exp \hat{r}_{\mathcal{P}}(\tau_2)} \\ &= \frac{\pi_1^{\text{SFT}}}{\pi_1^{\text{SFT}} + \pi_2^{\text{SFT}}} = \frac{6}{10}. \end{aligned}$$

Hence, $\pi_1^{\text{AIHF}} = \frac{10}{10+100}\pi_1^*(\hat{r}_{\mathcal{D}}) + \frac{100}{10+100}\pi_1^*(\hat{r}_{\mathcal{P}}) = \frac{56}{110}$. In this example, the RLHF policy estimator is again farthest from ground-truth, because it does not correctly dismiss the information provided by the demonstration data which is less informative than preference.

Numerical Example 2. Let us use an illustrative example to show that RLHF method will result in significant data under-utilization when the demonstration coverage is limited. Assume that there are 50 actions, each with a ground-truth reward defined by $r_i = \frac{1}{\sigma\sqrt{2\pi}}e^{-\frac{(\frac{i}{50}-\mu)^2}{2\sigma^2}}$, where $\mu = 0.5$ and $\sigma = 2$. Assume we can sample demonstration and preference from the ground truth reward distribution: demonstrations are sampled from the multinomial distribution, while preferences are sampled from the BTL model.

In an extreme scenario, let demonstrations cover actions 1 through 45, while preferences have full coverage across all actions. In the subsequent experiment, we initially sample 2000 demonstrations using the multinomial distribution $p_i = \frac{\exp r_i}{\sum_{j=1}^{45} \exp r_j}$, and obtain 200 preferences for each preference pair with $p(i \succ j) = \frac{\exp r_i}{\exp r_j + \exp r_i}$. We then calculate the optimal policy by solving the previously mentioned first order conditions, yielding the following result.

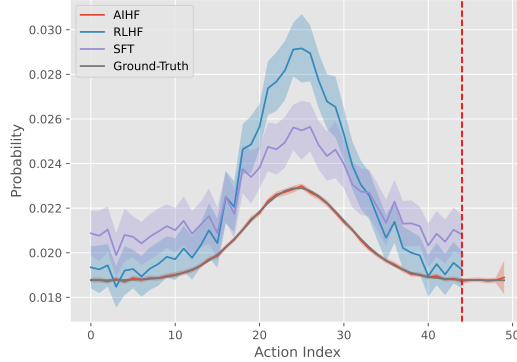


Figure 2: The optimal policy of RLHF, SFT, AIHF, and Ground-truth distribution. The left region of the red dotted line is included in the demonstration, while the right region is uncovered. We report the results with 100 random repeats.

From the result shown in Figure 2, we demonstrate that both SFT and RLHF transfer the weight from uncovered action to covered action when demonstration coverage is limited, as indicated by $\pi_{SFT}(a_{uncovered}) = 0$. Consequently, the weight of covered actions is significantly higher than the ground truth. However, this issue does not occur when jointly optimizing the demonstration and preference in the AIHF method.

5 Proposed Algorithm for AIHF Training

We are now ready to design algorithms for the proposed AIHF formulation (8). To begin with, first note that (8) takes a hierarchical form, and it belongs to the class of problem named *bi-level* optimization, first developed in the 70s [Fiacco and McCormick, 1990], and recently found many applications in machine learning [Wang et al., 2021, Liu et al., 2021, 2022]. Generically speaking, bi-level problems are not easy to optimize; more specifically, in (8), the upper-level problem (8a) is a function of *both* the lower-level optimal solution π_θ and the true parameter θ . It follows that a (stochastic) first-order algorithm for $L(\theta)$ involves some (potentially non-trivial) implicit gradient computation which often involves computing the Hessian matrix for the lower-level objective function. Fortunately, as we will show shortly, with some special choices of L_1 , L_2 , L_3 , one can design some simple and very efficient algorithms.

Throughout this section, we are searching for a good policy π_θ and a reward estimate $r(\cdot, \cdot; \theta)$ to align with human feedback, where the policy π_θ is an optimal solution w.r.t. the certain reward estimate $r(\cdot, \cdot; \theta)$ according to the policy optimization problem (3.4). Due to such optimal policy constraint w.r.t. one explicit reward estimate, we design an algorithm to solve such a single-stage,

bi-level problem which is different from DPO [Rafailov et al., 2023] that simply optimizes the fixed loss function (13) directly.

On a high level, the proposed algorithm alternates between a policy alignment step (which updates π with a fixed reward $r(\cdot, \cdot; \theta)$), and a reward alignment step (which updates θ using a stochastic gradient, a function of the demonstration and preference data). Next, we study these steps in detail.

Policy Alignment Step. From our earlier discussion, we know that when L_3 takes the form (10), the optimal policy (for a fixed reward) is given by (5). Of course, one cannot directly compute such an optimal solution due to the fact that both Q_θ and the normalization term are unknown. Therefore one can adopt the standard approaches such as the well-known proximal policy optimization (PPO) [Schulman et al., 2017] algorithm to obtain an approximate optimal policy. It is worth noting that, when considering $T = 1$, our discussion leading to (7) indicates the optimal policy takes a much simpler form. In this case, it is possible to consider simpler method than running PPO to obtain the optimal policy. One alternative way is to use a baseline estimated reward value to perform variance reduction Li et al. [2023], thus reducing the computational complexity.

It is important to note that, the point of the above discussion is that these different choices for solving the policy alignment problem can be incorporated into our overall approach.

Reward Alignment. In this step, we use a stochastic gradient-type algorithm to optimize $L(\theta)$. Towards this end, first observe that

$$\nabla L(\theta) = \alpha \nabla L_1(\pi_\theta) + \nabla L_2(\theta). \quad (26)$$

Clearly, regardless of the choice of L_2 , ∇L_2 is relatively easy to compute because the objective is directly related to θ since $L_2(\theta)$ can be regarded as one supervised learning loss and do not involve the optimal policy π_θ . In particular, we have the following expressions:

$$\nabla L_2^{\text{BTL}}(\theta) = \mathbb{E}_{(\tau_l \prec \tau_w) \sim \pi^P} \left[\nabla_\theta \log \left(\sigma(R(\tau_w; \theta) - R(\tau_l; \theta)) \right) \right]. \quad (27)$$

On the contrary, the computation of $\nabla L_1(\pi_\theta)$ is more involved, since L_1 depends on θ *implicitly* through the corresponding optimal policy π_θ . Fortunately, the following lemma indicates that this gradient has a simple and intuitive form as well.

Lemma 5.1 *Suppose that L_1 takes the form of the objective (1) for reward learning from demonstrations, and suppose that L_3 takes the form (10) with $c(\cdot)$ being the KL-divergence w.r.t. some initial policy π^0 . Then we have the following expression:*

$$\nabla_\theta L_1(\pi_\theta) = \mathbb{E}_{\tau \sim \pi^E, \tau' \sim \pi_\theta} [\nabla_\theta (R(\tau; \theta) - R(\tau'; \theta))] \quad (28)$$

where π_θ is the optimal policy given the reward model parameterized by θ , with the expression (5).

Intuitively, if the current policy π_θ has not matched π^E yet, then the reward should be improved by going towards the direction suggested by the expert trajectories, while *going away* from those generated by the current policy. Similar to the BTL model, from the gradient expression (28), it is clear that the optimization is toward the direction of increasing the gap between the reward of the real samples (demonstrations) and the synthetic ones (model generated continuations).

In practice, a few approximations need to be made to obtain a stochastic gradient of L_1 . First, similarly, as before, the precise expectation cannot be obtained because the ground truth policy

Algorithm 1: *Alignment with Integrated Human Feedback (AIHF)*

Input: Initialize reward parameter θ^0 and policy model π^0 , the stepsize of reward update η . Let \mathcal{P} , \mathcal{D}^E denote the preference and the demonstration data, respectively.
for Iteration $k = 0, 1, \dots, K - 1$ **do**
 Policy Alignment: Optimizing L_3 by RL subroutine, e.g. PPO, to obtain one improved policy π^{k+1}
 Data Sample I: Sample expert trajectories $\tau \sim \mathcal{D}^E$ and agent trajectories from $\tau' \sim \pi^{k+1}$
 Data Sample II: Sample preference pair $(\tau_l \prec \tau_w) \sim \mathcal{P}$
 Estimating Gradient: Calculate the estimator $g^k := \alpha g_1^k + g_2^k$ of $\nabla_\theta L(\theta_k) = \alpha \nabla_\theta L_1(\theta_k) + \nabla_\theta L_2(\theta_k)$
 Reward Alignment: $\theta^{k+1} := \theta^k + \eta g^k$
end for

π^E is unknown. Denote an offline demonstration dataset as $\mathcal{D}^E := \{\tau\}$, then one can replace the expectations $\mathbb{E}_{\tau \sim \pi^E}$ by $\mathbb{E}_{\tau \sim \mathcal{D}^E}$. Second, in the second expectation in (28), the trajectories τ' are sampled from π_θ , the optimal policy for a fixed reward parameterization by θ . This means that the *policy alignment* step has to identify the optimal policy π_θ first, which, due to limitations such as computational constraints, and non-linear parameterization, is generally not possible. Instead, we propose to sample from the *current* policy π^{k+1} obtained from the previous policy optimization step, where index k represents the iteration counter. The above two steps are summarized in Algorithm 1.

Let us remark on the gradient expression of the proposed algorithm. Here, we explain how to construct the gradient estimator g_1^k for $\nabla_\theta L_1(\theta_k)$ defined in (28) and g_2^k for $\nabla_\theta L_2(\theta_k)$ defined in (27). At iteration k , to estimate $\nabla_\theta L_1(\theta_k)$, we need to sample N expert trajectories τ^E from the expert demonstration dataset \mathcal{D}^E and N agent trajectories τ' from the policy π^{k+1} . Then the gradient estimator g_1^k can be constructed as: $g_1^k := \frac{1}{N} \sum_{i=1}^N [\nabla_\theta R(\tau_i; \theta) - \nabla_\theta R(\tau'_i; \theta)]$. Furthermore, through sampling M pairs of preference $(\tau_l \prec \tau_w)$, we can further construct the gradient estimator of $\nabla_\theta L_2(\theta_k)$ as: $g_2^k = \sum_{i=1}^M \nabla_\theta \log \left(\sigma(R(\tau_{i,w}; \theta) - R(\tau_{i,l}; \theta)) \right)$. It is interesting to note that, although the demonstration data is used, in the final algorithm, the gradient is always in contrastive form. The difference is that for the demonstration data, it is compared with its own model generation, while for preference data, two preference data is compared.

Before we close this section, let us remark on the computational complexity of the proposed algorithm. Note that our algorithm is motivated by a class of popular algorithms in bi-level optimization, where the upper-level and lower-level problems are updated alternately using stochastic optimization [Hong et al., 2020].

Specifically, one only needs to perform one (or a few steps) of policy optimization step (such as PPO) to obtain an improved π^{k+1} before moving to the next iteration.

As demonstrated in our subsequent numerical results, the computational complexity of our method is comparable or sometimes even lower as compared to their sequential optimization counterparts such as RLHF. In our numerical results, we show that the proposed algorithm AIHF can achieve a comparable performance as RLHF while performing less policy optimization steps.

6 Experiments

In this section, we present numerical results for the proposed method. More specifically, we intend to address the following questions: 1) How are the data efficiency and model improvement efficiency (w.r.t. the KL divergence violation) of our proposed method compared with other baselines? 2) Can

we achieve the same convergence results after integrating the three stages into one stage? 3) And finally, how much does demonstration help in reward learning in AIHF? To answer these questions, we consider several applications of the alignment problem. In this section, we show the numerical results for large language model alignment in the Helpful and Harmless (HH) dataset [Bai et al., 2022] and robotics control problem in MuJoCo Todorov et al. [2012]. In the appendix, we have another set of experiment where the goal is to align the language model so that it generates movie reviews with positive sentiment on IMDB dataset [Maas et al., 2011].

6.1 MuJoCo Tasks

In MuJoCo, we consider several robotic control tasks with continuous action space. We evaluate the performance of our proposed algorithm on aligning robot behaviors with provided demonstrations and preference data. After the robot training stage, we leverage the ground-truth reward function from the environment to evaluate the performance.

Data. Following the similar data generation pipeline in Brown et al. [2019], we generate the expert demonstrations and preference dataset as follows. We first train an expert agent by leveraging the ground-truth reward function and the popular Soft Actor-Critic (SAC) algorithm Haarnoja et al. [2018], which is developed to solve policy optimization problems with continuous action space. During the training process, we save the policy checkpoints and collect 30k samples from each checkpoint. To achieve precise control of dataset quality, we categorize the data collected into three different classes: low-, medium-, and high-quality datasets according to the performance of the checkpoints. Then we combine the low- and medium-quality data as the preference dataset and use high-quality as demonstration data.

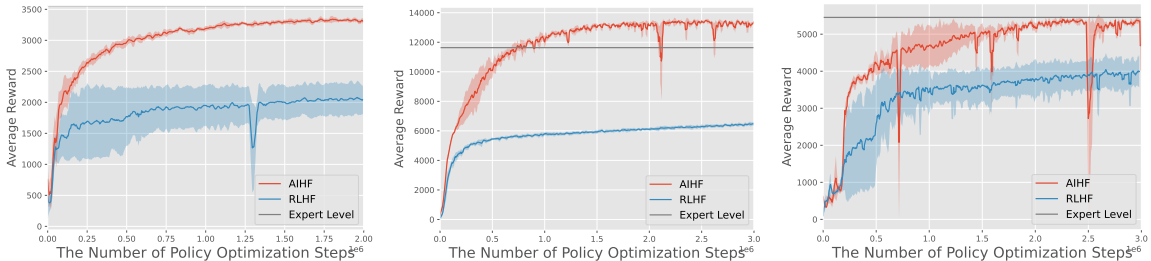


Figure 3: **Left: Hopper Environment Middle: HalfCheetah Environment Right: Walker2d Environment;** AIHF (orange) vs RLHF(blue); results are averaged over 3 independent runs. We use 10k demonstrations and 20k preferences. The RLHF curve is initialized from a policy pre-trained by BC; the AIHF from a random policy. The performance is compared against the # of SAC steps performed (for AIHF each policy alignment performs 5k steps of SAC.)

Results. We show that AIHF is able to integrate (insufficient amount of) demonstration data and (not-so-high-quality) preference data to generate high-quality policy, and it significantly outperforms the RLHF. In Fig. 3, we observe that due to the limited number of demonstration data Ross and Bagnell [2010], Zeng et al. [2022b], BC fails to provide a high-performing initialization for finetuning for RLHF. Moreover, since the preference data quality is only of low-to-medium quality, the RL step based on the learned reward model fails to significantly boost the fine-tuning performance. In contrast, clearly the proposed AIHF can effectively integrate preferences and demonstrations, leading to a more robust reward function and consequently, a high-quality policy.

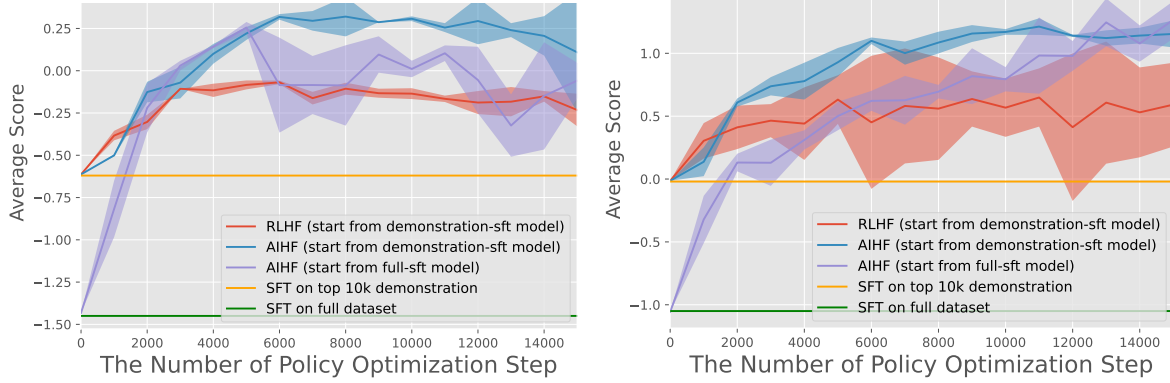


Figure 4: Helpfulness-controlled Generation. Left: Results on 160M models, Right: Results on 1B models. We record the average scores of AIHF and RLHF on the Anthropic-HH test dataset, reporting the results across three different trials.

6.2 LLM Task

In the experiment utilizing the HH dataset, we aim to generate helpful continuations through aligning large language models with human preference. We compare our proposed algorithm *AIHF* which updates reward and policy iteratively, with the standard RLHF benchmark. Additionally, $L_2(\cdot)$ is chosen to be L_2^{BTL} defined (11), and L_1 , L_3 are chosen similarly as in MuJoCo experiment. More settings are listed in the Appendix A.2. For evaluation, we use the existing reward model PKU-ALIGNMENT/BEAVER-7B-V3.0-REWARD¹ for the helpful continuation generation; use the existing sentiment classifier LVWERRA/DISTILBERT-IMDB² as the ground truth reward model for the movie review generation task.

Data. We divide the training dataset of HH dataset into three different subsets: demonstration dataset, preference dataset, and RL training dataset. We employed the reward model PKU-Alignment/beaver-7b-v3.0-reward Dai et al. [2023], Ji et al. [2024] to filter the datasets. Specifically, We selected the 10k responses with the highest reward score as our demonstration dataset and utilized an additional 10,000 pairwise comparisons as preference data. The remaining prompts were then used to run the RL algorithm.

Setting. For the HH dataset, We first fine-tune the language models (Pythia-160M / Pythia-1B) Biderman et al. [2023] through supervised fine-tuning over all chosen responses from the HH dataset for 1 epoch, we call it full-SFT model and use it as our base model. Moreover, we supervised fine-tuned the language model using the selected top 10k "chosen" responses and named it the demonstration-SFT model. For the reward model, we use ELEUTHERAI/PYTHIA-1.4B³ for both 160m and 1B policy as its base model.

Results. We observe that the proposed approach AIHF performs effectively when initiated from both the demonstration-SFT model and the full-SFT model. As shown in Fig. 4, utilizing the same data, the AIHF algorithms can eventually outperform RLHF irrespective of the initial model. Furthermore, according to the numerical results as shown in Fig. 5, compared with the RLHF benchmark, we see that the proposed AIHF algorithm has smaller deviation from the base model. This benefit of the AIHF approach is due to the fact that we incorporate the maximum likelihood

¹<https://huggingface.co/PKU-Alignment/beaver-7b-v3.0-reward>

²<https://huggingface.co/lvwerra/distilbert-imdb>

³<https://huggingface.co/EleutherAI/pythia-1.4b>

IRL objective for both reward learning and policy learning. In this case, both reward model and policy model will be trained to align with the demonstrations, which are also used in the training process of the SFT stage. Fig. 5 shows AIHF effectively maintains the policy close to the initial model. This advantage can be partially attributed to Eq. (8a), as the inclusion of the demonstration regularization term encourages the alignment with the demonstration distribution, thus bringing better performance without significant deviation from the initial model. The win rate (ratio of samples where the reward of our model’s generation is higher than the model compared) provided by Fig 5 further shows the superiority of the proposed approach.

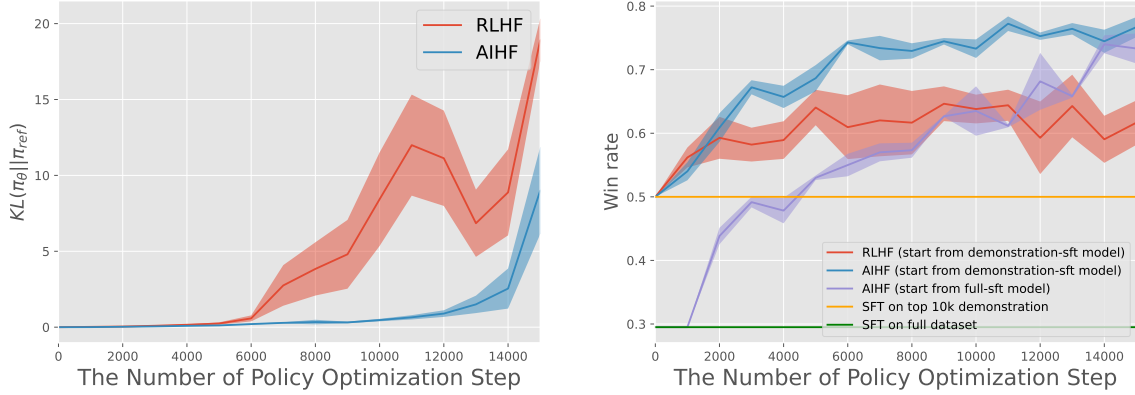


Figure 5: Helpfulness-controlled Generation on 1B models. Left: KL divergence to the Demonstration-SFT policy, Right: win rate of AIHF and RLHF over the Demonstration-SFT model.

7 Conclusion

In this work, we study the alignment problem when diverse data sources from human feedback are available. Furthermore, we have developed an algorithmic framework that can integrate both expert demonstration and pairwise comparison data from human feedback to learn the reward functions for further guiding policy learning/model fine-tuning in the alignment pipeline. Through extensive evaluations on robotic control tasks and large language model alignment tasks, we demonstrate that our proposed method can outperform existing benchmarks on alignment tasks and is able to recover a better reward model to guide policy learning. One limitation is that our framework only incorporates expert demonstrations and pairwise comparisons for reward learning. In fact, it is promising to extend the information sources from human feedback/behaviors to further strengthen the reward learning/policy fine-tuning stages. For example, one can utilize precise comparisons and demonstrations from different aspects to further learn a powerful reward model in order to support better alignment quality.

References

Saurabh Arora and Prashant Doshi. A survey of inverse reinforcement learning: Challenges, methods and progress. *Artificial Intelligence*, 297:103500, 2021.

- Mohammad Gheshlaghi Azar, Mark Rowland, Bilal Piot, Daniel Guo, Daniele Calandriello, Michal Valko, and Rémi Munos. A general theoretical paradigm to understand learning from human preferences. *arXiv preprint arXiv:2310.12036*, 2023.
- Yuntao Bai, Andy Jones, Kamal Ndousse, Amanda Askell, Anna Chen, Nova DasSarma, Dawn Drain, Stanislav Fort, Deep Ganguli, Tom Henighan, et al. Training a helpful and harmless assistant with reinforcement learning from human feedback. *arXiv preprint arXiv:2204.05862*, 2022.
- Marc G Bellemare, Salvatore Candido, Pablo Samuel Castro, Jun Gong, Marlos C Machado, Subhodeep Moitra, Sameera S Ponda, and Ziyu Wang. Autonomous navigation of stratospheric balloons using reinforcement learning. *Nature*, 588(7836):77–82, 2020.
- Christopher Berner, Greg Brockman, Brooke Chan, Vicki Cheung, Przemysław Dębiak, Christy Dennison, David Farhi, Quirin Fischer, Shariq Hashme, Chris Hesse, et al. Dota 2 with large scale deep reinforcement learning. *arXiv preprint arXiv:1912.06680*, 2019.
- Stella Biderman, Hailey Schoelkopf, Quentin Gregory Anthony, Herbie Bradley, Kyle O’Brien, Eric Hallahan, Mohammad Aflah Khan, Shivanshu Purohit, USVSN Sai Prashanth, Edward Raff, et al. Pythia: A suite for analyzing large language models across training and scaling. In *International Conference on Machine Learning*, pages 2397–2430. PMLR, 2023.
- Erdem Bıyık, Dylan P Losey, Malayandi Palan, Nicholas C Landolfi, Gleb Shevchuk, and Dorsa Sadigh. Learning reward functions from diverse sources of human feedback: Optimally integrating demonstrations and preferences. *The International Journal of Robotics Research*, 41(1):45–67, 2022.
- Pavlo R Blavatsky and Ganna Pogrebna. Models of stochastic choice and decision theories: Why both are important for analyzing decisions. *Journal of Applied Econometrics*, 25(6):963–986, 2010.
- Michael Bloem and Nicholas Bambos. Infinite time horizon maximum causal entropy inverse reinforcement learning. In *53rd IEEE conference on decision and control*, pages 4911–4916. IEEE, 2014.
- Ralph Allan Bradley and Milton E Terry. Rank analysis of incomplete block designs: I. the method of paired comparisons. *Biometrika*, 39(3/4):324–345, 1952.
- Daniel Brown, Wonjoon Goo, Prabhat Nagarajan, and Scott Niekum. Extrapolating beyond suboptimal demonstrations via inverse reinforcement learning from observations. In *International conference on machine learning*, pages 783–792. PMLR, 2019.
- Josef Dai, Xuehai Pan, Ruiyang Sun, Jiaming Ji, Xinbo Xu, Mickel Liu, Yizhou Wang, and Yaodong Yang. Safe rlhf: Safe reinforcement learning from human feedback. *arXiv preprint arXiv:2310.12773*, 2023.
- Christian Daniel, Malte Viering, Jan Metz, Oliver Kroemer, and Jan Peters. Active reward learning. In *Robotics: Science and systems*, volume 98, 2014.
- Anthony V Fiacco and Garth P McCormick. *Nonlinear programming: sequential unconstrained minimization techniques*. SIAM, 1990.

- Johannes Fischer, Christoph Eyberg, Moritz Werling, and Martin Lauer. Sampling-based inverse reinforcement learning algorithms with safety constraints. In *2021 IEEE/RSJ International Conference on Intelligent Robots and Systems (IROS)*, pages 791–798. IEEE, 2021.
- Drew Fudenberg, Ryota Iijima, and Tomasz Strzalecki. Stochastic choice and revealed perturbed utility. *Econometrica*, 83(6):2371–2409, 2015.
- Tuomas Haarnoja, Aurick Zhou, Pieter Abbeel, and Sergey Levine. Soft actor-critic: Off-policy maximum entropy deep reinforcement learning with a stochastic actor. In *International conference on machine learning*, pages 1861–1870. PMLR, 2018.
- Joey Hejna and Dorsa Sadigh. Inverse preference learning: Preference-based rl without a reward function. *arXiv preprint arXiv:2305.15363*, 2023.
- Jiwoo Hong, Noah Lee, and James Thorne. Orpo: Monolithic preference optimization without reference model. *arXiv preprint arXiv:2403.07691*, 2024.
- Mingyi Hong, Hoi-To Wai, Zhaoran Wang, and Zhuoran Yang. A two-timescale framework for bilevel optimization: Complexity analysis and application to actor-critic. *arXiv preprint arXiv:2007.05170*, 2020.
- Borja Ibarz, Jan Leike, Tobias Pohlen, Geoffrey Irving, Shane Legg, and Dario Amodei. Reward learning from human preferences and demonstrations in atari. *Advances in neural information processing systems*, 31, 2018.
- Jiaming Ji, Mickel Liu, Josef Dai, Xuehai Pan, Chi Zhang, Ce Bian, Boyuan Chen, Ruiyang Sun, Yizhou Wang, and Yaodong Yang. Beavertails: Towards improved safety alignment of llm via a human-preference dataset. *Advances in Neural Information Processing Systems*, 36, 2024.
- Kaiyi Ji, Junjie Yang, and Yingbin Liang. Bilevel optimization: Convergence analysis and enhanced design. In *International Conference on Machine Learning*, pages 4882–4892. PMLR, 2021.
- Dmitry Kalashnikov, Alex Irpan, Peter Pastor, Julian Ibarz, Alexander Herzog, Eric Jang, Deirdre Quillen, Ethan Holly, Mrinal Kalakrishnan, Vincent Vanhoucke, et al. Scalable deep reinforcement learning for vision-based robotic manipulation. In *Conference on Robot Learning*, pages 651–673. PMLR, 2018.
- Prashant Khanduri, Siliang Zeng, Mingyi Hong, Hoi-To Wai, Zhaoran Wang, and Zhuoran Yang. A near-optimal algorithm for stochastic bilevel optimization via double-momentum. *Advances in Neural Information Processing Systems*, 34, 2021.
- Jens Kober and Jan Peters. Policy search for motor primitives in robotics. *Advances in neural information processing systems*, 21, 2008.
- Jan Leike, David Krueger, Tom Everitt, Miljan Martic, Vishal Maini, and Shane Legg. Scalable agent alignment via reward modeling: a research direction. *arXiv preprint arXiv:1811.07871*, 2018.
- Sergey Levine, Zoran Popovic, and Vladlen Koltun. Nonlinear inverse reinforcement learning with gaussian processes. *Advances in neural information processing systems*, 24, 2011.

- Ziniu Li, Tian Xu, Yushun Zhang, Yang Yu, Ruoyu Sun, and Zhi-Quan Luo. Remax: A simple, effective, and efficient method for aligning large language models. *arXiv preprint arXiv:2310.10505*, 2023.
- Zeyi Liao and Huan Sun. Amplegcg: Learning a universal and transferable generative model of adversarial suffixes for jailbreaking both open and closed llms. *arXiv preprint arXiv:2404.07921*, 2024.
- Risheng Liu, Jiaxin Gao, Jin Zhang, Deyu Meng, and Zhouchen Lin. Investigating bi-level optimization for learning and vision from a unified perspective: A survey and beyond. *IEEE Transactions on Pattern Analysis and Machine Intelligence*, 44(12):10045–10067, 2021.
- Risheng Liu, Pan Mu, Xiaoming Yuan, Shangzhi Zeng, and Jin Zhang. A general descent aggregation framework for gradient-based bi-level optimization. *IEEE Transactions on Pattern Analysis and Machine Intelligence*, 45(1):38–57, 2022.
- Tianqi Liu, Yao Zhao, Rishabh Joshi, Misha Khalman, Mohammad Saleh, Peter J Liu, and Jialu Liu. Statistical rejection sampling improves preference optimization. *arXiv preprint arXiv:2309.06657*, 2023.
- Zhihan Liu, Miao Lu, Shenao Zhang, Boyi Liu, Hongyi Guo, Yingxiang Yang, Jose Blanchet, and Zhaoran Wang. Provably mitigating overoptimization in rlhf: Your sft loss is implicitly an adversarial regularizer. *arXiv preprint arXiv:2405.16436*, 2024.
- Andrew Maas, Raymond E Daly, Peter T Pham, Dan Huang, Andrew Y Ng, and Christopher Potts. Learning word vectors for sentiment analysis. In *Proceedings of the 49th annual meeting of the association for computational linguistics: Human language technologies*, pages 142–150, 2011.
- Volodymyr Mnih, Koray Kavukcuoglu, David Silver, Andrei A Rusu, Joel Veness, Marc G Bellemare, Alex Graves, Martin Riedmiller, Andreas K Fidjeland, Georg Ostrovski, et al. Human-level control through deep reinforcement learning. *nature*, 518(7540):529–533, 2015.
- Tetsuro Morimura, Mitsuki Sakamoto, Yuu Jinnai, Kenshi Abe, and Kaito Air. Filtered direct preference optimization. *arXiv preprint arXiv:2404.13846*, 2024.
- Vivek Myers, Erdem Biyik, Nima Anari, and Dorsa Sadigh. Learning multimodal rewards from rankings. In *Conference on Robot Learning*, pages 342–352. PMLR, 2022.
- Long Ouyang, Jeffrey Wu, Xu Jiang, Diogo Almeida, Carroll Wainwright, Pamela Mishkin, Chong Zhang, Sandhini Agarwal, Katarina Slama, Alex Ray, et al. Training language models to follow instructions with human feedback. *Advances in Neural Information Processing Systems*, 35: 27730–27744, 2022.
- Malayandi Palan, Nicholas C Landolfi, Gleb Shevchuk, and Dorsa Sadigh. Learning reward functions by integrating human demonstrations and preferences. *arXiv preprint arXiv:1906.08928*, 2019.
- Peter S Park, Simon Goldstein, Aidan O’Gara, Michael Chen, and Dan Hendrycks. Ai deception: A survey of examples, risks, and potential solutions. *arXiv preprint arXiv:2308.14752*, 2023.

- Ethan Perez, Sam Ringer, Kamilė Lukošiuūtė, Karina Nguyen, Edwin Chen, Scott Heiner, Craig Pettit, Catherine Olsson, Sandipan Kundu, Saurav Kadavath, et al. Discovering language model behaviors with model-written evaluations. *arXiv preprint arXiv:2212.09251*, 2022.
- Dean A Pomerleau. Alvin: An autonomous land vehicle in a neural network. *Advances in neural information processing systems*, 1, 1988.
- Rafael Rafailov, Archit Sharma, Eric Mitchell, Stefano Ermon, Christopher D Manning, and Chelsea Finn. Direct preference optimization: Your language model is secretly a reward model. *arXiv preprint arXiv:2305.18290*, 2023.
- Stéphane Ross and Drew Bagnell. Efficient reductions for imitation learning. In *Proceedings of the thirteenth international conference on artificial intelligence and statistics*, pages 661–668. JMLR Workshop and Conference Proceedings, 2010.
- John Schulman, Filip Wolski, Prafulla Dhariwal, Alec Radford, and Oleg Klimov. Proximal policy optimization algorithms. *arXiv preprint arXiv:1707.06347*, 2017.
- Nisan Stiennon, Long Ouyang, Jeffrey Wu, Daniel Ziegler, Ryan Lowe, Chelsea Voss, Alec Radford, Dario Amodei, and Paul F Christiano. Learning to summarize with human feedback. *Advances in Neural Information Processing Systems*, 33:3008–3021, 2020.
- Emanuel Todorov, Tom Erez, and Yuval Tassa. Mujoco: A physics engine for model-based control. In *2012 IEEE/RSJ international conference on intelligent robots and systems*, pages 5026–5033. IEEE, 2012.
- Masatoshi Uehara, Nathan Kallus, Jason D Lee, and Wen Sun. Refined value-based offline rl under realizability and partial coverage. *arXiv preprint arXiv:2302.02392*, 2023.
- Runzhong Wang, Zhigang Hua, Gan Liu, Jiayi Zhang, Junchi Yan, Feng Qi, Shuang Yang, Jun Zhou, and Xiaokang Yang. A bi-level framework for learning to solve combinatorial optimization on graphs. *Advances in Neural Information Processing Systems*, 34:21453–21466, 2021.
- Markus Wulfmeier, Peter Ondruska, and Ingmar Posner. Maximum entropy deep inverse reinforcement learning. *arXiv preprint arXiv:1507.04888*, 2015.
- Shusheng Xu, Wei Fu, Jiaxuan Gao, Wenjie Ye, Weilin Liu, Zhiyu Mei, Guangju Wang, Chao Yu, and Yi Wu. Is dpo superior to ppo for llm alignment? a comprehensive study. *arXiv preprint arXiv:2404.10719*, 2024.
- Zheng Yuan, Hongyi Yuan, Chuanqi Tan, Wei Wang, Songfang Huang, and Fei Huang. Rrhf: Rank responses to align language models with human feedback without tears. *arXiv preprint arXiv:2304.05302*, 2023.
- Siliang Zeng, Mingyi Hong, and Alfredo Garcia. Structural estimation of markov decision processes in high-dimensional state space with finite-time guarantees. *arXiv preprint arXiv:2210.01282*, 2022a.
- Siliang Zeng, Chenliang Li, Alfredo Garcia, and Mingyi Hong. Maximum-likelihood inverse reinforcement learning with finite-time guarantees. *Advances in Neural Information Processing Systems*, 2022b.

Zhengyuan Zhou, Michael Bloem, and Nicholas Bambos. Infinite time horizon maximum causal entropy inverse reinforcement learning. *IEEE Transactions on Automatic Control*, 63(9):2787–2802, 2017.

Banghua Zhu, Hiteshi Sharma, Felipe Vieira Frujeri, Shi Dong, Chenguang Zhu, Michael I Jordan, and Jiantao Jiao. Fine-tuning language models with advantage-induced policy alignment. *arXiv preprint arXiv:2306.02231*, 2023.

Brian D Ziebart. *Modeling purposeful adaptive behavior with the principle of maximum causal entropy*. Carnegie Mellon University, 2010.

Brian D Ziebart, J Andrew Bagnell, and Anind K Dey. The principle of maximum causal entropy for estimating interacting processes. *IEEE Transactions on Information Theory*, 59(4):1966–1980, 2013.

A Appendix / supplemental material

A.1 Proof of Lemma 5.1

Proof. Here, under a reward parameter θ and the corresponding optimal policy π_θ of (5).

Moreover, under a fixed reward parameter θ , we have defined the optimal policy π_θ as below:

$$\pi_\theta := \arg \max_{\pi} \mathbb{E}_{\tau^A \sim \pi} \left[\sum_{t=0}^{\infty} \gamma^t \left(r(s_t, a_t; \theta) + \beta \mathcal{D}_{KL} \left(\pi(\cdot | s_t) || \pi^0(\cdot | s_t) \right) \right) \right].$$

According to Uehara et al. [2023], the optimal policy π_θ of (10) has the closed form expression as below:

$$\pi_\theta(a|s) = \frac{\pi^0(a|s) \exp \left(\frac{Q_\theta(s, a; \theta)}{\beta} \right)}{\sum_{\tilde{a} \in \mathcal{A}} \pi^0(\tilde{a}|s) \exp \left(\frac{Q_\theta(s, \tilde{a}; \theta)}{\beta} \right)}, \quad \forall s \in \mathcal{S}, a \in \mathcal{A}. \quad (29)$$

Based on the closed form of π_θ , we can also obtain the closed form of V_θ as following:

$$V_\theta(s) := \beta \log \left(\sum_{a \in \mathcal{A}} \pi^0(a|s) \exp \left(\frac{Q_\theta(s, a)}{\beta} \right) \right). \quad (30)$$

Then we can re-write the demonstration loss $L_1(\theta)$ as below:

$$\begin{aligned}
L_1(\theta) &= \mathbb{E}_{\tau^E \sim \pi^E} \left[\sum_{t=0}^{\infty} \gamma^t \log \pi_{\theta}(a_t | s_t) \right] \\
&= \mathbb{E}_{\tau^E \sim \pi^E} \left[\sum_{t=0}^{\infty} \gamma^t \log \left(\frac{\pi^0(a_t | s_t) \exp \left(\frac{Q_{\theta}(s_t, a_t)}{\beta} \right)}{\sum_{\tilde{a} \in \mathcal{A}} \pi^0(\tilde{a} | s_t) \exp \left(\frac{Q_{\theta}(s_t, \tilde{a})}{\beta} \right)} \right) \right] \\
&= \mathbb{E}_{\tau^E \sim \pi^E} \left[\sum_{t=0}^{\infty} \gamma^t \left(\log \left(\pi^0(a_t | s_t) \exp \left(\frac{Q_{\theta}(s_t, a_t)}{\beta} \right) \right) - \log \left(\sum_{\tilde{a} \in \mathcal{A}} \pi^0(\tilde{a} | s_t) \exp \left(\frac{Q_{\theta}(s_t, \tilde{a})}{\beta} \right) \right) \right) \right] \\
&= \mathbb{E}_{\tau^E \sim \pi^E} \left[\sum_{t=0}^{\infty} \gamma^t \left(\log \pi^0(a_t | s_t) + \frac{Q_{\theta}(s_t, a_t)}{\beta} - \log \left(\sum_{\tilde{a} \in \mathcal{A}} \pi^0(\tilde{a} | s_t) \exp \left(\frac{Q_{\theta}(s_t, \tilde{a})}{\beta} \right) \right) \right) \right] \\
&= \frac{1}{\beta} \mathbb{E}_{\tau^E \sim \pi^E} \left[\sum_{t=0}^{\infty} \gamma^t \left(\beta \log \pi^0(a_t | s_t) + Q_{\theta}(s_t, a_t) - \beta \log \left(\sum_{\tilde{a} \in \mathcal{A}} \pi^0(\tilde{a} | s_t) \exp \left(\frac{Q_{\theta}(s_t, \tilde{a})}{\beta} \right) \right) \right) \right] \\
&= \frac{1}{\beta} \mathbb{E}_{\tau^E \sim \pi^E} \left[\sum_{t=0}^{\infty} \gamma^t \left(\beta \log \pi^0(a_t | s_t) + Q_{\theta}(s_t, a_t) - V_{\theta}(s_t) \right) \right] \tag{31}
\end{aligned}$$

Then we can take gradient of $L_1(\theta)$ w.r.t. the reward parameter θ , we have the following expression:

$$\begin{aligned}
\nabla L_1(\theta) &:= \frac{1}{\beta} \mathbb{E}_{\tau^E \sim \pi^E} \left[\sum_{t=0}^{\infty} \gamma^t \left(\nabla_{\theta} \beta \log \pi^0(a_t | s_t) + \nabla_{\theta} Q_{\theta}(s_t, a_t) - \nabla_{\theta} V_{\theta}(s_t) \right) \right] \\
&= \frac{1}{\beta} \mathbb{E}_{\tau^E \sim \pi^E} \left[\sum_{t=0}^{\infty} \gamma^t \left(\nabla_{\theta} Q_{\theta}(s_t, a_t) - \nabla_{\theta} V_{\theta}(s_t) \right) \right] \\
&= \frac{1}{\beta} \mathbb{E}_{\tau^E \sim \pi^E} \left[\sum_{t=0}^{\infty} \gamma^t \left(\nabla_{\theta} r(s_t, a_t; \theta) + \gamma \nabla_{\theta} V_{\theta}(s_{t+1}) - \nabla_{\theta} V_{\theta}(s_t) \right) \right] \\
&= \frac{1}{\beta} \mathbb{E}_{\tau^E \sim \pi^E} \left[\sum_{t=0}^{\infty} \gamma^t \nabla_{\theta} r(s_t, a_t; \theta) \right] - \frac{1}{\beta} \mathbb{E}_{s_0 \sim \rho} \left[\nabla_{\theta} V_{\theta}(s_0) \right] \tag{32}
\end{aligned}$$

In order to calculate the expression of $\nabla L_1(\theta)$, we further derive the expression of $\nabla_{\theta} V_{\theta}(s_0)$:

$$\begin{aligned}
\nabla_{\theta} V_{\theta}(s_0) &= \nabla_{\theta} \left(\beta \log \left(\sum_{a \in \mathcal{A}} \pi^0(a | s_0) \exp \left(\frac{Q_{\theta}(s_0, a)}{\beta} \right) \right) \right) \\
&= \beta \sum_{a \in \mathcal{A}} \frac{\pi^0(a | s_0) \exp \left(\frac{Q_{\theta}(s_0, a)}{\beta} \right)}{\sum_{a \in \mathcal{A}} \pi^0(a | s_0) \exp \left(\frac{Q_{\theta}(s_0, a)}{\beta} \right)} \frac{\nabla_{\theta} Q_{\theta}(s_0, a)}{\beta} \\
&= \mathbb{E}_{a \sim \pi_{\theta}(\cdot | s_0)} \left[\nabla_{\theta} Q_{\theta}(s_0, a) \right] \\
&= \mathbb{E}_{a_0 \sim \pi_{\theta}(\cdot | s_0), s_1 \sim P(\cdot | s_0, a_0)} \left[\nabla_{\theta} r(s_0, a_0; \theta) + \gamma \nabla_{\theta} V_{\theta}(s_1) \right] \\
&= \mathbb{E}_{\tau^A \sim \pi_{\theta}} \left[\sum_{t=0}^{\infty} \gamma^t \nabla_{\theta} r(s_t, a_t; \theta) \mid s_0 \right] \tag{33}
\end{aligned}$$

By plugging (33) into (32), we obtain the following expression:

$$\nabla L_1(\theta) = \frac{1}{\beta} \mathbb{E}_{\tau^E \sim \pi^E} \left[\sum_{t=0}^{\infty} \gamma^t \nabla_{\theta} r(s_t, a_t; \theta) \right] - \frac{1}{\beta} \mathbb{E}_{\tau^A \sim \pi_{\theta}} \left[\sum_{t=0}^{\infty} \gamma^t \nabla_{\theta} r(s_t, a_t; \theta) \right] \quad (34)$$

A.2 Experiment Setup and Additional Result

A.2.1 MuJoCo Tasks

In MuJoCo, we consider several robotic control tasks with continuous action space. We evaluate the performance of our proposed algorithm on aligning robot behaviors with provided demonstrations and preference data. After the robot training stage, we leverage the ground-truth reward function from the environment to evaluate the performance.

Data. Following the similar data generation pipeline in Brown et al. [2019], we generate the expert demonstrations and preference dataset as follows. We first train an expert agent by leveraging the ground-truth reward function and the popular Soft Actor-Critic (SAC) algorithm Haarnoja et al. [2018], which is developed to solve policy optimization problems with continuous action space. During the training process, we save the policy checkpoints and collect 30k samples from each checkpoint. To achieve precise control of dataset quality, we categorize the data collected into three different classes: low-, medium-, and high-quality datasets according to the performance of the checkpoints. Then we combine the low- and medium-quality data as the preference dataset and use high-quality as demonstration data.

Settings. We set $L_1(\cdot)$ using the likelihood objective (9), $L_2(\cdot)$ as the BTL objective (11), and L_3 as KL-regularized objective given in (10). We implement the RLHF Brown et al. [2019] using the following 3 steps: (i) utilize the demonstration dataset to pre-train the policy using behavior cloning (BC) Pomerleau [1988]; (ii) conduct reward learning using preference data; (iii) implement the SAC for policy fine-tuning. In the proposed AIHF, the policy π^0 is initiated with a random policy, and the policy optimization problem is also solved using SAC.

In all Mujoco experiments, we assess the performance of benchmark algorithms on Hopper, HalfCheetah, and Walker2d from OpenAI Gym. To ensure a fair comparison, we utilize an open-source implementation of SAC⁴ as the foundational RL algorithm for all methods. Regarding the choice of the penalty function $c(\cdot)$, since our proposed pipeline, AIHF, initiates with a random policy where $\pi(a|s)$ follows a uniform distribution, the kl penalty function is reduced to an entropy function.

In SAC, both the policy network and Q network are (64, 64) MLPs with ReLU activation function, and the step size is set to $3 * 10^{-3}$, we parameterize the reward function by a (64, 64) MLPs with ReLU activation function. For the reward network, we use Adam as the optimizer, and the step size is set to be $1 * 10^{-4}$.

The quality of the preference dataset and demonstration dataset are listed as follows Tab. 1:

In the following sections, we include additional details about language alignment experiments.

A.2.2 Sentiment-Controlled Generation

Dataset Generation: In the IMDb sentiment completion task, we generate the demonstrations and preference datasets using the following procedure. Initially, we train a Language Model by employing

⁴<https://github.com/openai/spinningup>

Dataset Task	Non-prefer Data	Prefer Data	Demonstration Data
Hopper-v2	2345.20 \pm 329.93	3024.63 \pm 40.52	3559.61 \pm 73.12
HalfCheetah-v2	7226.37 \pm 126.88	9434.42 \pm 1315.13	11635.42 \pm 236.51
Walker2d-v2	3952.60 \pm 444.45	5091.71 \pm 291.73	5453.41 \pm 71.07

Table 1: The quality of preference and demonstration.

the ground-truth reward function DISTILBERT-IMDB and the Proximal Policy Optimization (PPO) algorithm on 30% of the training dataset for IMDb. Throughout the training process, we save the policy checkpoint every 500 PPO steps. Subsequently, we select an additional 40% of the training dataset and generate a response for each prompt for each checkpoint. According to the evaluation score of each generation, we categorize the data collected into different classes: low-, medium-, and high-quality datasets, then we combine low-quality and medium-quality as preference datasets, and use high-quality as demonstration datasets. We show the average score of each dataset in 3,

Training: After acquiring the preference and demonstration datasets, we train the proposed algorithm AIHF and baselines on the remaining 30% of prompts from the training dataset. We evaluate the performance of each algorithm using the test datasets for IMDb and HH, along with their corresponding ground truth reward functions. For the GPU resources, we use 8 \times A10 for all the experiments. Please refer to Table 2 for detailed hyperparameters and model initialization setting, and Table 3 for the quality of the preference and demonstration datasets we synthesize.

Results: Policy Quality. We find that the proposed approach works well when either preference or demonstration data, or both, are limited. From the 6, we see that by using the same amount of data (10k preference, 10k demonstration), AIHF-based algorithms achieve faster convergence than their RLHF and DPO counterparts. Next, in Fig. 7, we show that policy learned using AIHF generates higher-quality continuations (measured by higher reward scores), as compared with those generated by RLHF, across a number of different combinations of preference and demonstration data size. and the size of preference data can significantly affect the quality of the estimated policy of RLHF, while it only affects the convergence speed of AIHF.

Results: Distribution Mismatch. We show that AIHF is able to alleviate the distribution mismatch between the generated trajectories by the policy, and the data that the learned reward model is able to rank. To evaluate the extend of such mismatch, we use the following three steps: (1) use 1k preference, 1k demonstration to train policy and reward model for RLHF and AIHF ; (2) for a given set of prompts from test dataset, use RLHF and AIHF to perform generation; (3) use the trained reward models to rate the generation; (4) compare with the score generated by the ground truth reward LVWERRA/DISTILBERT-IMDB. Fig. 8 illustrates that the reward score distribution produced by AIHF aligns closely with that of the ground truth reward, whereas that generated by RLHF exhibits a poor match. These results show that the reward model learned by AIHF is able to correctly evaluate the generation produced by the final policy.

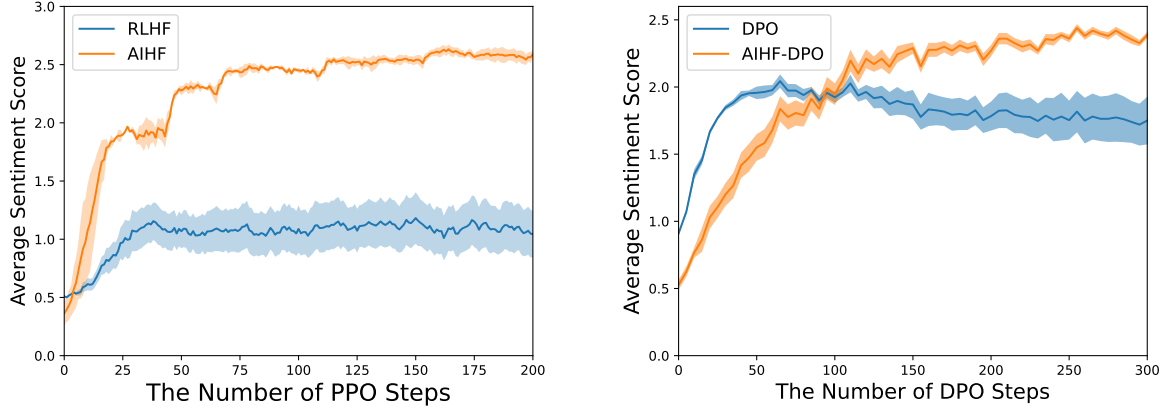


Figure 6: **IMDb Sentiment-controlled Generation. Left: AIHF vs RLHF; Right: AIHF-DPO vs DPO;** These represent limited data regimes with 1k preference, and 1k demonstration. Results are averaged over 3 independent runs. The RLHF and DPO curves are initialized from the SFT policy; the AIHF-based algorithms are initialized from a random policy. The achieved reward is compared against the # of PPO (resp, DPO) steps performed (for AIHF each policy alignment performs 20 steps of PPO).

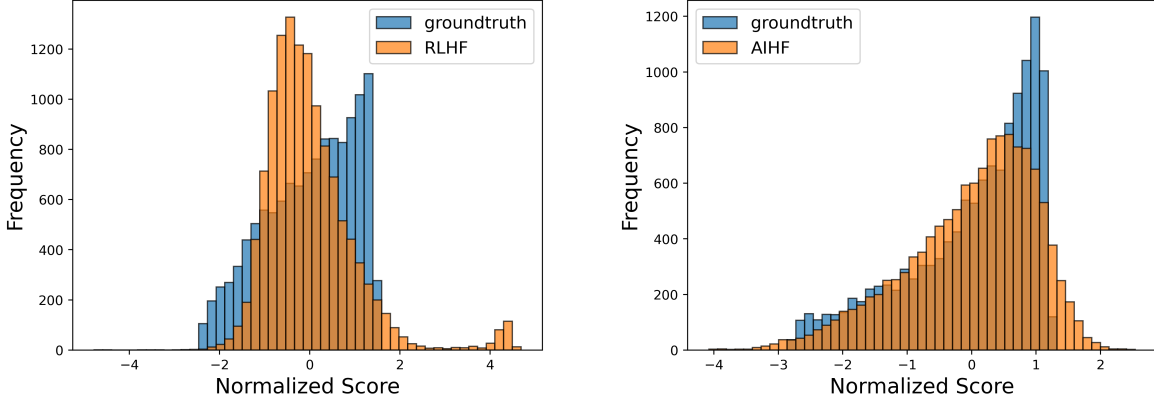
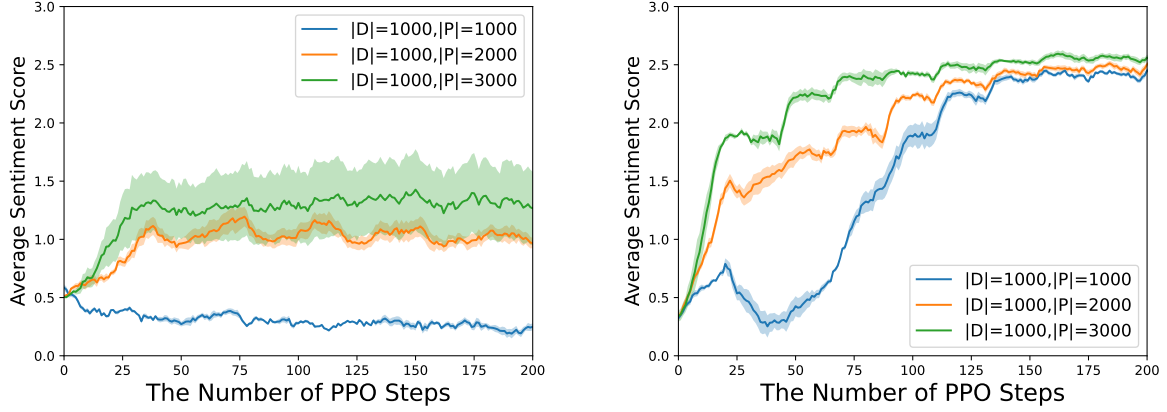
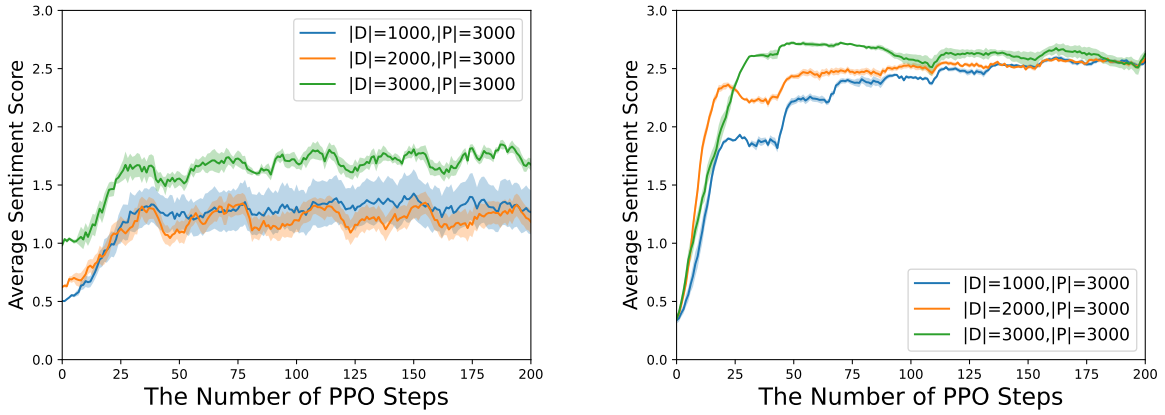


Figure 8: Comparison of the distribution of reward score generated by the trained reward models, and the ground truth reward model. RLHF vs ground truth (left); AIHF vs ground truth (right).

From Fig.9, our proposed algorithm AIHF could obtain higher rewards than baseline methods in the IMDb setting for almost all KL values. Although AIHF might get a low score from the ground truth reward model in the earlier step, AIHF would get a higher reward with more iteration and optimization steps. This indicates that with the mix of demonstration data and preference data, we could prevent the policy from known issues of reward hacking, especially when the policy learned more human-aligned features beyond base models (high KL value). Moreover, AIHF is persistent in the number of preference data, presenting that AIHF could still gain benefit from the limited preference data in more optimization steps as long as the demonstration data is high quality enough.



(a) RLHF (left) vs AIHF (right); Fix demonstration number to 1000, gradually increase preference number.



(b) RLHF (left) vs AIHF (right); Fix preference number to 3k, gradually increase demonstration number.

Figure 7: **IMDb Sentiment-controlled Generation RLHF vs AIHF** ; (a) different demonstration data size; (b) preference data.

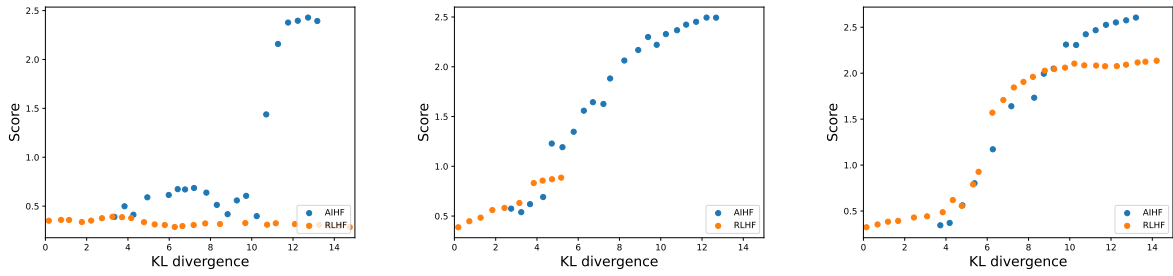


Figure 9: **The frontier of expected reward vs KL to the reference policy in IMDb dataset. fix the demonstration number to 3k** Left: Using 1k preference; Middle: Using 2k preferences; Right: Using 3k preference

task hyperparameters	IMDb Secontrolled Generation	H&H Alignment
policy model	GPT2	PYTHIA-160M & PYTHIA-1B
reward model	GPT2	PYTHIA-1.4B
reward learning rate	1e-5	1e-5
policy learning rate	1.41e-5	1e-6
reward batch size	128	8
policy batch size	256	4
sample temperature	1.00	1.00
policy update times per iteration	20	6000
reward update times per iteration	12	20

Table 2: Hyperparameters of AIHF. H&H refers to Helpful and Harmless.

Dataset Task	Non-prefer Data	Prefer Data	Demonstration Data
IMDb	0.27 ± 0.51	1.13 ± 0.42	2.23 ± 0.13
Helpful and Harmless	-1.61 ± 0.24	-1.12 ± 0.17	-0.82 ± 0.05

Table 3: The quality of preference and demonstration.

In Fig.10, we show the converge curves of AIHF-DPO vs vanilla DPO in different combinations of preference and demonstration data size. Moreover, we observe that AIHF-DPO is stable over all different settings, while DPO is unstable and its performance slowly decreases over time.

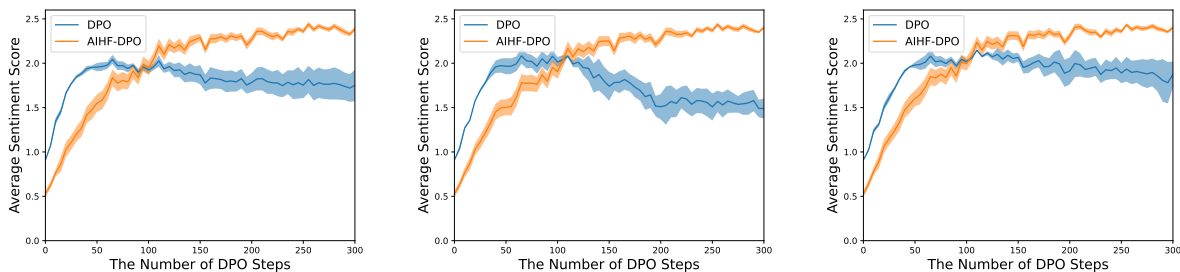


Figure 10: **DPO vs AIHF-DPO** Left: 1k Demonstration 1k Preference, Middle:1k Demonstration 2k Preference Right:1k Demonstration 3k Preference.

A.2.3 Helpfulness-Controlled Generation

Results: Reward Distribution. Further, in Fig. 11, we show the overall reward distribution of the continuation, we can observe the distribution of AIHF and RLHF have some overlap in low-quality continuation, however, AIHF can generate more high-quality continuations compared to RLHF, which shows that joint optimization can more effectively align the policy model with the

demonstration distribution.

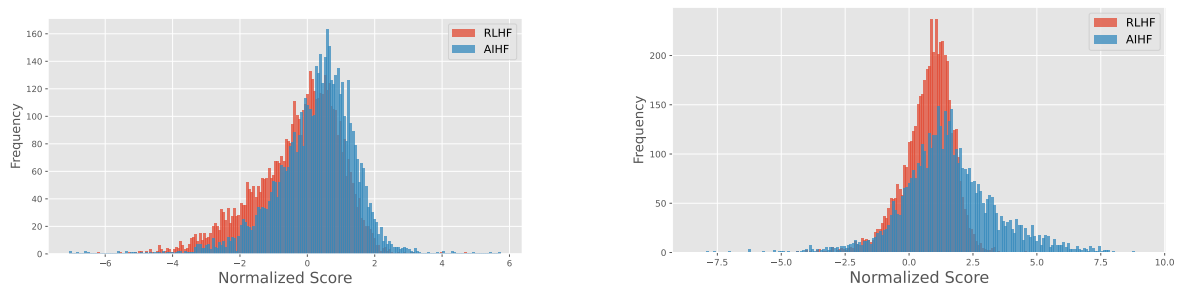


Figure 11: **The Reward Distribution of Helpfulness-controlled Generation. Left: Result on 160m model, Right: Results on 1B model**, This figure reports the reward distribution of generation evaluated by PKU-Alignment/beaver-7b-v3.0-reward for AIHF and RLHF.